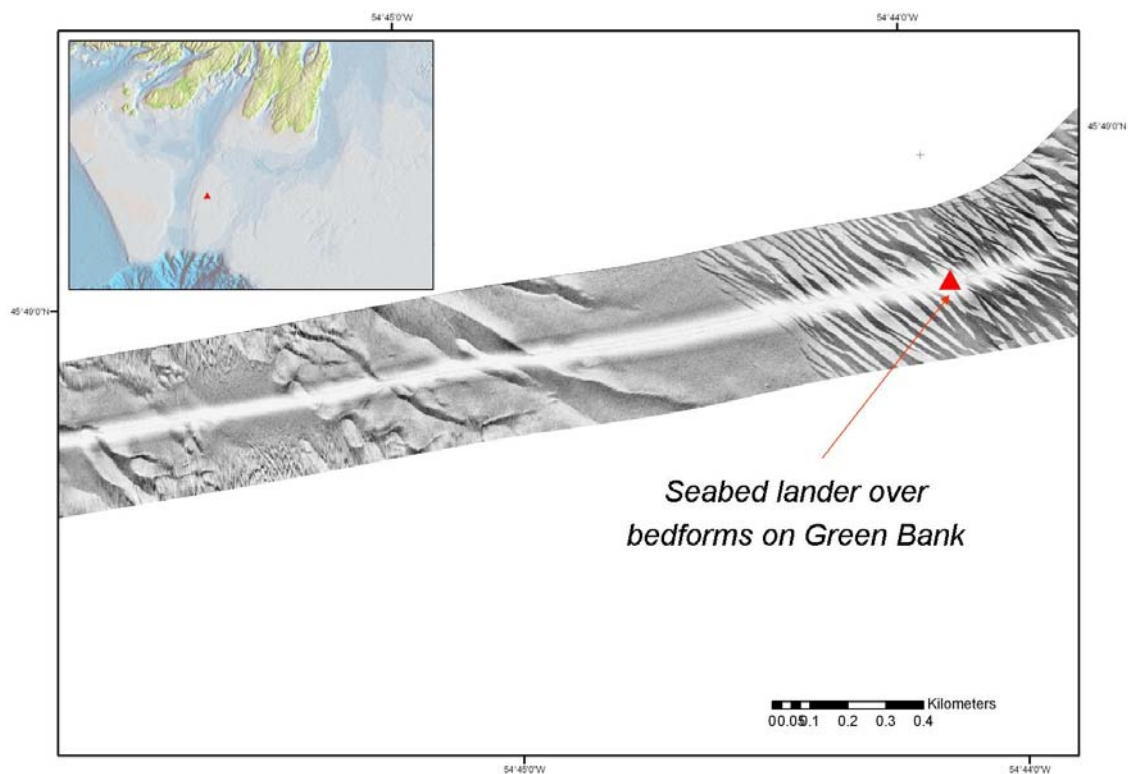




**GEOLOGICAL SURVEY OF CANADA
OPEN FILE 6744**

**Hydrodynamics and Seabed Stability Observations
From 2007 Lander Deployment on Green Bank, western
Grand Banks**

M.Z. Li, R.H. Prescott and A. Robertson



2011



Natural Resources
Canada

Ressources naturelles
Canada

Canada



**GEOLOGICAL SURVEY OF CANADA
OPEN FILE 6744**

**Hydrodynamics and Seabed Stability Observations
From 2007 Lander Deployment on Green Bank, western
Grand Banks**

M.Z. Li, R.H. Prescott and A. Robertson

2011

©Her Majesty the Queen in Right of Canada 2011

doi:10.4095/288035

This publication is available from the Geological Survey of Canada Bookstore
(http://gsc.nrcan.gc.ca/bookstore_e.php).

It can also be downloaded free of charge from GeoPub (<http://geopub.nrcan.gc.ca/>).

Recommended citation:

Li, M. Z., Prescott, R.H. and Robertson, A., 2011. Hydrodynamics and Seabed Stability Observations From 2007 Lander Deployment on Green Bank, western Grand Banks; Geological Survey of Canada, Open File 6744, 54 p.
doi:10.4095/288035

TABLE OF CONTENTS

1. INTRODUCTION	<u>1</u>
2. INSTRUMENTATION AND DEPLOYMENT LOCATION	<u>3</u>
2.1 Deployment location	<u>3</u>
2.2 Instrumentation	<u>3</u>
2.3 Sensor Performance and Data Quality	<u>7</u>
3. HYDRODYNAMICS OBSERVATIONS	<u>8</u>
3.1 Wave and Current Parameters and Sediment Suspension	<u>8</u>
3.2 Relative impact of near-bed mean current and wave oscillation	<u>11</u>
3.3 Near-bed flows during storms	<u>11</u>
4. SEDIMENT TRANSPORT AND SEABED STABILITY OBSERVATIONS	<u>15</u>
4.1 Bedforms	<u>15</u>
4.2 Sediment suspension	<u>15</u>
5. PREDICTIONS BY SEDTRANS96	<u>20</u>
6. SUMMARY	<u>26</u>
ACKNOWLEDGEMENT	<u>28</u>
REFERENCES	<u>29</u>

APPENDICES

Appendix 1: Burst-averaged wave, current and sediment suspension parameters for the 2007 Green Bank deployment.

Appendix 2: Bottom boundary layer dynamics parameters predicted by SEDTRANS96 for 2007 Green Bank deployment.

Appendix 3: Ripple metrics and sediment transport parameters predicted by SEDTRANS96 for 2007 Green Bank deployment.

Hydrodynamics and Seabed Stability Observations From 2007 Lander Deployment on Green Bank, western Grand Banks

Michael Z. Li¹, Robert H. Prescott², and Angus Robertson¹

¹Geological Survey of Canada (Atlantic)
Bedford Institute of Oceanography
P. O. Box 1006, Dartmouth, Nova Scotia, B2Y 4A2

²Prescott and Zou Consulting
6 Glenn Dr.
Halifax, Nova Scotia, B3M 2B9

1. INTRODUCTION

The sediment and substrate on the sea floor of the continental shelf and slope of Atlantic Canada is influenced by strong wave oscillation, wind-driven currents during storms, and other oceanic currents. The seabed instability caused by these processes can be potential geohazards or constraints to offshore hydrocarbon developments and other engineering and energy projects (cables, tidal and wind farms, etc.). Since early 1990s, the Geological Survey of Canada - Atlantic (GSCA), through government funding and partnership with industry, has conducted comprehensive research on combined-flow bottom boundary layer dynamics and sediment transport processes, seabed scouring and mobile layer depth during storms, and the morphodynamics of sand ridges and other bedforms on Sable Island Bank, Scotian Shelf (Li et al., 1994; Amos et al., 1996; Li et al., 1997; Li and Amos, 1999; Li et al., 1999; King, 2002; Li et al., 2003; Smyth et al., 2003; Li and King, 2007; Li et al., in press). The interest of the oil and gas industry has shifted to deep water prospects on upper Scotian slope and on the Newfoundland and Labrador margins in recent years. Several shelf-crossing pipelines have also been considered for moving the offshore products to land and then to market. Regional knowledge of seabed scouring and bedform distribution and mobility on the Grand Banks and the Newfoundland margin, is needed for safe design and operation of seabed facilities and for the selection of the optimal pipeline corridors.

To address the seabed scouring and bedform mobility issues on the Grand Banks, GSCA instrumented lander RALPH was deployed over a field of megaripples and sand waves on Green Bank, western Grand Banks (Figure 1), in the winter of 2007 to collect in situ sediment dynamics data for improved understanding of nearbed wave and current forcing and sediment and bedform mobility at this site. This report describes the seabed instrumentation and presents the preliminary results of hydrodynamics and seabed stability observations obtained from this lander deployment.

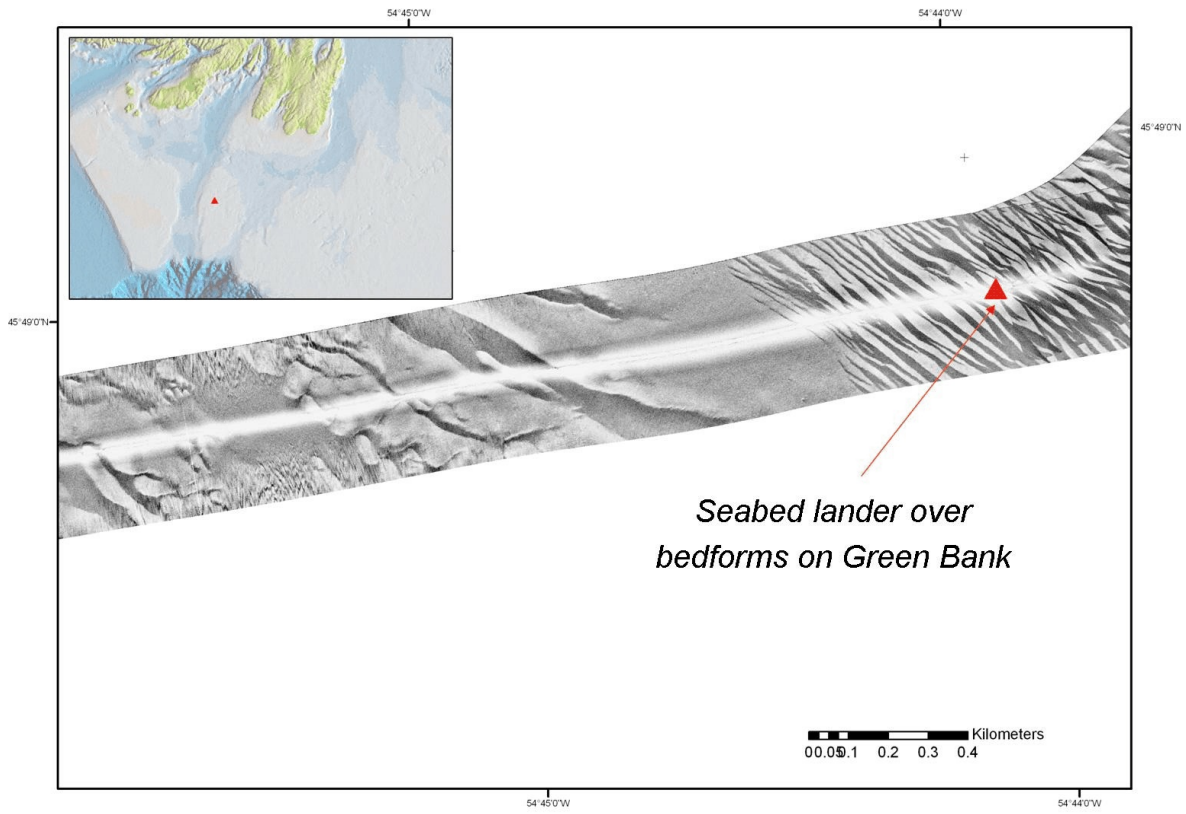


Figure 1 Location of 2007 Green Bank lander deployment superimposed on a sidescan sonogram.

2. INSTRUMENTATION AND DEPLOYMENT LOCATION

2.1 Deployment location

The GSCA instrumented platform RALPH was deployed on Green Bank, western Grand Banks, from 7 December 2007 (yearday 341) to 19 January 2008 for a period of 43 days. The deployment (Expedition 2007103) and recovery (Expedition 2008101) were both via a ship of opportunity on CCGS Hudson. The site was over a field of megaripples on western central Green Bank at 45° 48.2939'N, 54° 46.3273'W in about 71 m depth. Figure 1 demonstrates the geographic location of the deployment and precise position of the lander superimposed on a sidescan sonagram. A surface (0-2 cm) and a mixed bulk sample were collected using a van Veen grab sampler on the deployment expedition. The surface sample was submitted to the GSCA Sedimentology Laboratory (SedLab) for grain size analysis which showed that the bottom sediment at the deployment site is composed of medium sand with a mean grain size $D = 0.31$ mm. The bulk sample was also processed and will be used in the lander sensor calibration in the future.

2.2 Instrumentation

RALPH is an autonomous instrumented platform (Figure 2) for long-term in-situ measurements of wave-current dynamics and seabed responses in marine environments. Detailed descriptions of the system have been given by Heffler (1996) and Li et al. (1999).

Table 1 summarizes the sensors on RALPH and the variables they are intended to measure for this deployment. The key sensors include: 2 ALEC electro-magnetic current meters (EMCM); Nobska time-travel current meter MAVS3D, Nortek AquaDopp Acoustic Doppler Current Profiler (ADCP), 6 Optical Backscatter Sensors (OBS), one Acoustic Backscatter Sensor (ABS), Imagenex sector-scanning rotary pencil-beam (IMPen) and fan-beam (IMFan) sonars, and a Sony Digital Video camera (BurstCam). The top plan view of the positions of these sensors on the RALPH quad frame is shown in Figure 3. The reference origin of the X and Y is the center of the vertical leg near the fan beam sonar. With the fan beam sonar at the upper left corner, X positive is to the right, Y positive is to the top and Z positive is upward from the seabed. The RALPH heading (Y positive) was 315° in magnetic north. The magnetic declination of 19° west was not corrected in data processing. Thus all directions in this report are magnetic north readings.

The essential sensors on RALPH (pressure, compass, and OBS) were programmed to burst sample for 15 minutes duration every 2 hours at a frequency of 2 Hz. Corresponding to each data burst, the ABS logged data for 3.8 minutes at the frequency of 4 Hz. The Imagenex pencil-beam sonar was programmed to scan a 5 m profile for every burst, followed by the fan-beam sonar that collected a 20 m range image with 288° sector width. The digital video camera (BurstCam) was programmed to take a 2 s recording at the beginning and end of each 15 minute burst. The BurstCam lens was set at wide angle and auto focus. The Nobska MAVS3D travel time current meter was mounted pointing downward and set to sample at 5 Hz for 15 minutes every two

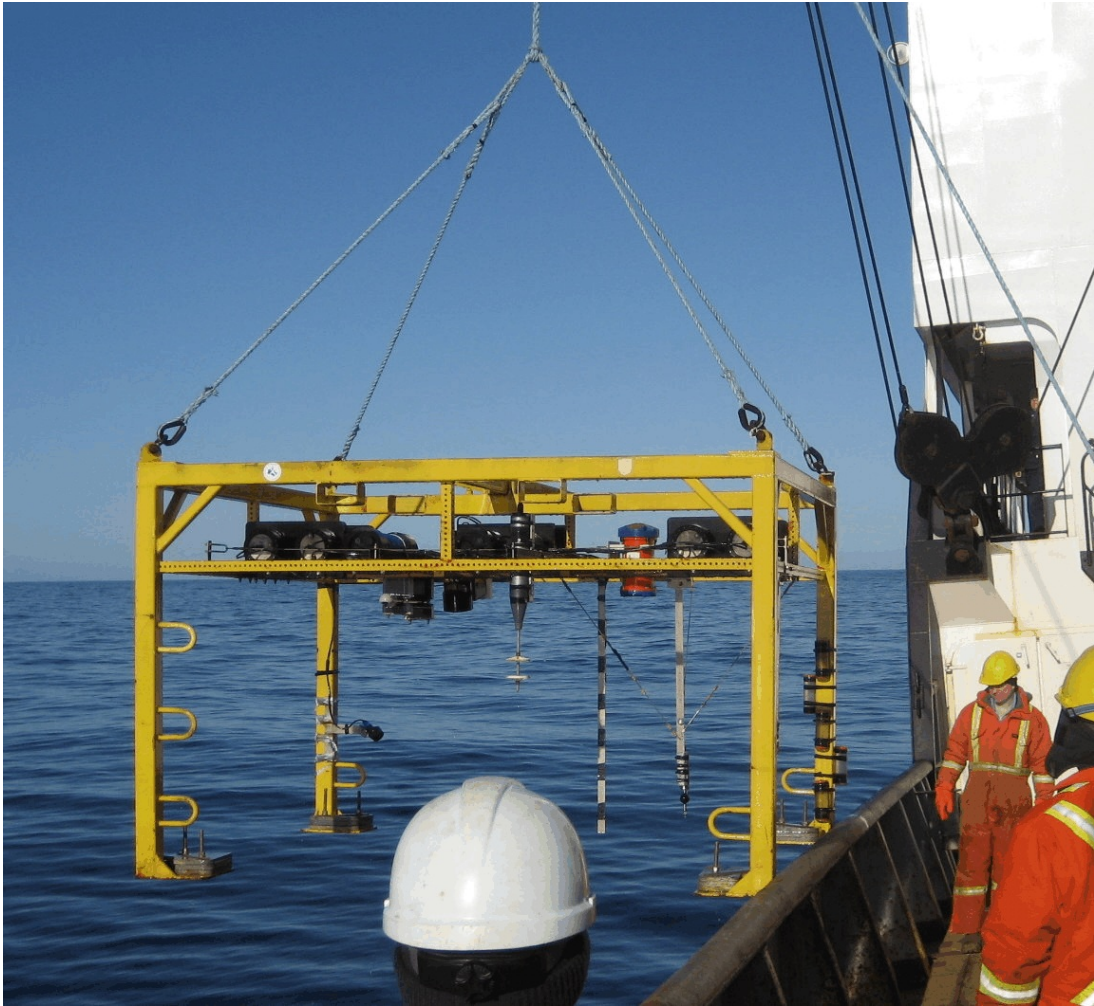


Figure 2 Photographic imagery of the sediment dynamics instrumented seabed lander RALPH.

Table 1 Sensor descriptions and positions on the RALPH frame. The abbreviation of sensors is given in the text. See Fig. 3 for the plan view of sensor positions.

Sensor	Variable Measured	Position (X,Y,Z in cm)
Pressure Sensor	depth; wave height	138,-89,156
Compass/Tilt	direction; tilt;	134,-105,152
ALEC EMCM 1 (Serial 273) 2 (Serial 273)	velocity profile	227,90,28 227,143,48
Nobska Current Meter MAVS3D	current and turbulence	160,190,100
Nortek ADCP	current profiles	97,150,130
OBS 1 (brown) 2 (red) 3 (orange) 4 (yellow) 5 (green) 6 (blue)	suspended sediment concentration	166,-74,13 166,-74,34 166,-74,52 166,-74,72 166,-74,92 166,-74,111
ABS (serial 2180)	seabed elevation; suspended sediment concentration profiles	111,-29,132
Imagenex sonars Pencil beam Fan beam	bedform bedform	112,-3,134 -10,10,159
Sony DV Camera BurstCam	bedform and sed. transport mode	107,-53,133

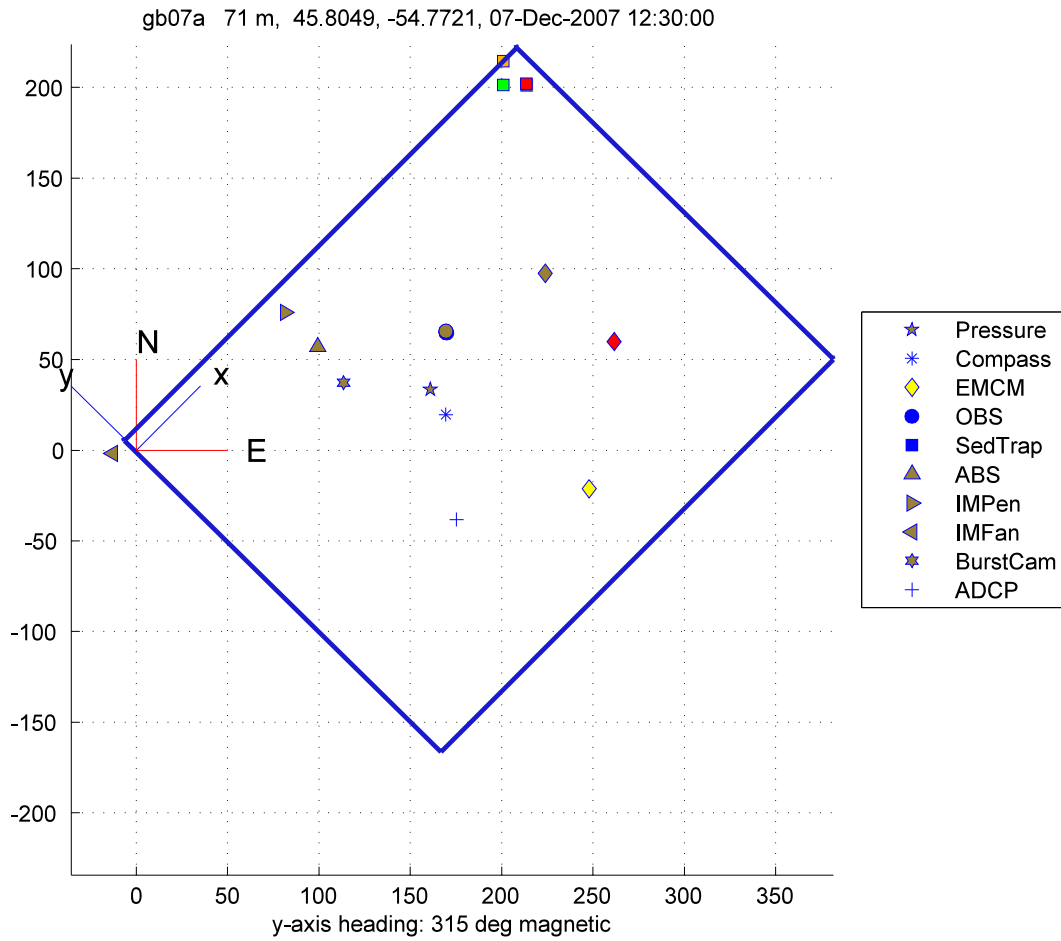


Figure 3 The top plan view of the positions of sensors on the RALPH platform. See text and Table 1 for full sensor definitions and positions.

hours. Both of the ALEC electro-magnetic current meters were set to run for 5 minutes every 2 hours at 1 Hz. The Nortek AquaDopp ADCP was positioned downward looking and set to record every hour a 20-minute averaged velocity profile sampled with a 1 Hz ping rate (i.e. measure velocity profiles for 20 minutes at 1 Hz every hour). The vertical resolution of the current profiles was 10 cm. Immediately following the current profiling, the instrument was set to measure waves by recording velocity and pressure for 17 minutes at 2 Hz every hour using an 80 cm cell size.

In the past, Ralph's pressure and velocity measurement from a set of four Marsh McBirney EMCM's were triggered and logged synchronously by the main Ralph controller. The processing for wave direction, which requires precise correlation of pressure and velocity, was done using these synchronous pressure and velocity data. The set of four EMCMs was damaged during a previous deployment and replaced with two independent ALEC EMCM's, the Nobska MAVS 3D acoustic current meter, and a Nortek ADCP profiler. These new sensors are all completely autonomous and they each have their own clock. Due to clock error, they do not sample at exactly the same time. Fortunately, both the MAVS and the Nortek ADCP have their own pressure gauge, so these pressure records are synchronous with their corresponding velocity measurements and there is no need to correlate the velocity with Ralph's main pressure record. The wave direction processing for this deployment was done using the pressure and velocity data from just the MAVS3D current meter. All these autonomous sensors were mounted on the frame separately, with careful attention to the alignment of the instruments' velocity axes relative to Ralph's x and y axes. Detailed descriptions of timing and alignment issues are given in Prescott (2008).

2.3 Sensor Performance and Data Quality

ALEC EMCM and MAVS current meters were mounted at 30, 50, and 100 cm above the bed respectively. The usual high sample rate measurement of current was not available at 70 cm height. However burst-mean current at this height was covered by the ADCP profile data. On the whole, the hydrodynamic data is of better quality than any previous Ralph deployment, and should permit estimates of shear stresses and turbulence parameters by several different methods.

This was the maiden deployment for the newly acquired Nobska MAVS 3D acoustic current meter. There were no problems at all with this instrument. It had 5 times the sample rate of the ALEC EMCMs, enough memory for a longer burst length and also longer deployment duration, and the important addition of the vertical velocity component. Its high quality pressure gauge eliminates the need for clock drift correction in the wave parameter computation process. It also has its own attitude sensors, temperature sensor, and compass. The 3-component velocity measurement allows for Reynold's stress and inertial dissipation estimates of bed shear stress.

The downward looking AquaDopp acoustic Doppler current profiler successfully recorded vertical profiles of 20-minute mean horizontal velocity. The high-frequency wave-mode recording was also successful. ABS1 (at 1 MHz) recorded bi-hourly for 20 days with no serious

problems. The overview of the OBS data did not find any new problems with the data. However the distribution function for the whole experiment shows that baseline drift leading to unphysical negative concentrations is still an issue. Calibration of acoustic and optical backscatter sensors using in situ sediment samples has not yet been done. Calibration coefficients derived for the fine sand from the 2007 Northeast Channel deployment were used to convert the ABS and OBS recordings to suspended sediment concentration in engineering unit (g/l or mg/l).

Both Imagex sonars performed flawlessly. The old problem of the fan-beam head stalling and losing count of stepper motor steps has been fixed. During storms, there are radial streaks caused by intermittent attenuation by clouds of suspended sediment. The pencil beam completed all scans as expected. The resolution limitation imposed by the oblique footprint of the beam on the seafloor makes it difficult to judge the height of small bedforms using automated bottom detection, but larger bedforms can be discerned.

RALPH's pitch, roll, and compass heading are plotted in Figure 4 in comparison with the recorded significant wave height. Since this deployment spanned New Years Day, the yeardays (YD) greater than 365 are days in January 2010. The changes of roll and pitch are less than 3 degrees for the duration of the deployment (approximately 40 days). The variation of the compass heading is less than 6 degrees. There was a change of 2 degrees in compass heading associated with the storm on the year-day 353 of 2007, but no apparent changes in roll and pitch were observed for this and all other storms. These observations indicate that the lander was stable during this field experiment.

3. HYDRODYNAMICS OBSERVATIONS

3.1 Wave and Current Parameters and Sediment Suspension

Through preliminary processing of the Green Bank 2007 RALPH data, calibration coefficients were applied and burst mean wave, current and sediment concentration parameters were obtained (Prescott, 2008). The burst-averaged wave, current and sediment suspension parameters for the 2007 Green Bank deployment are listed in Appendix 1. The time series of mean water depth h , mean velocity at 100 cm above seabed U_{100} , significant wave height H_s , wave period T_p , and suspended sediment concentration measured at about 50 cm above seabed are plotted in Figure 5.

The depth data in Fig. 5a clearly demonstrate the dominant semi-diurnal tides on Green Bank with a maximum tidal range of about 2 m. Several storms were recorded (Fig. 5c). The significant wave heights and wave periods in these storms ranged 3-8.5 m and 8-14 s respectively. The waves during the significant storms generally travelled to the north or northeast. The magnitude of the near-bed mean currents was generally less than 25 cm/s under fair-weather conditions, presumably mostly due to tidal current, but increased to a maximum

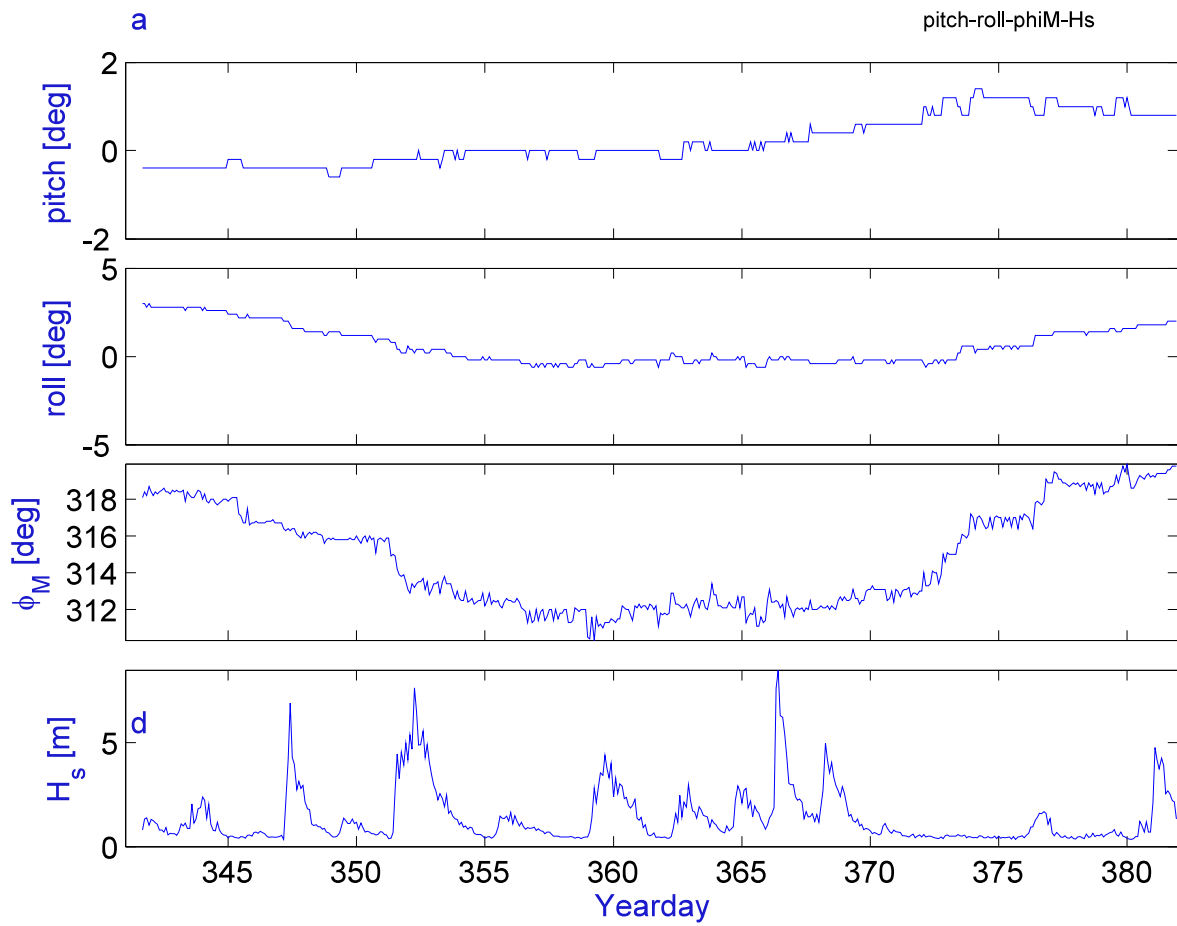


Figure 4 Time series of RALPH's pitch, roll, and compass heading (Φ_M) in comparison with the recorded significant wave height H_s .

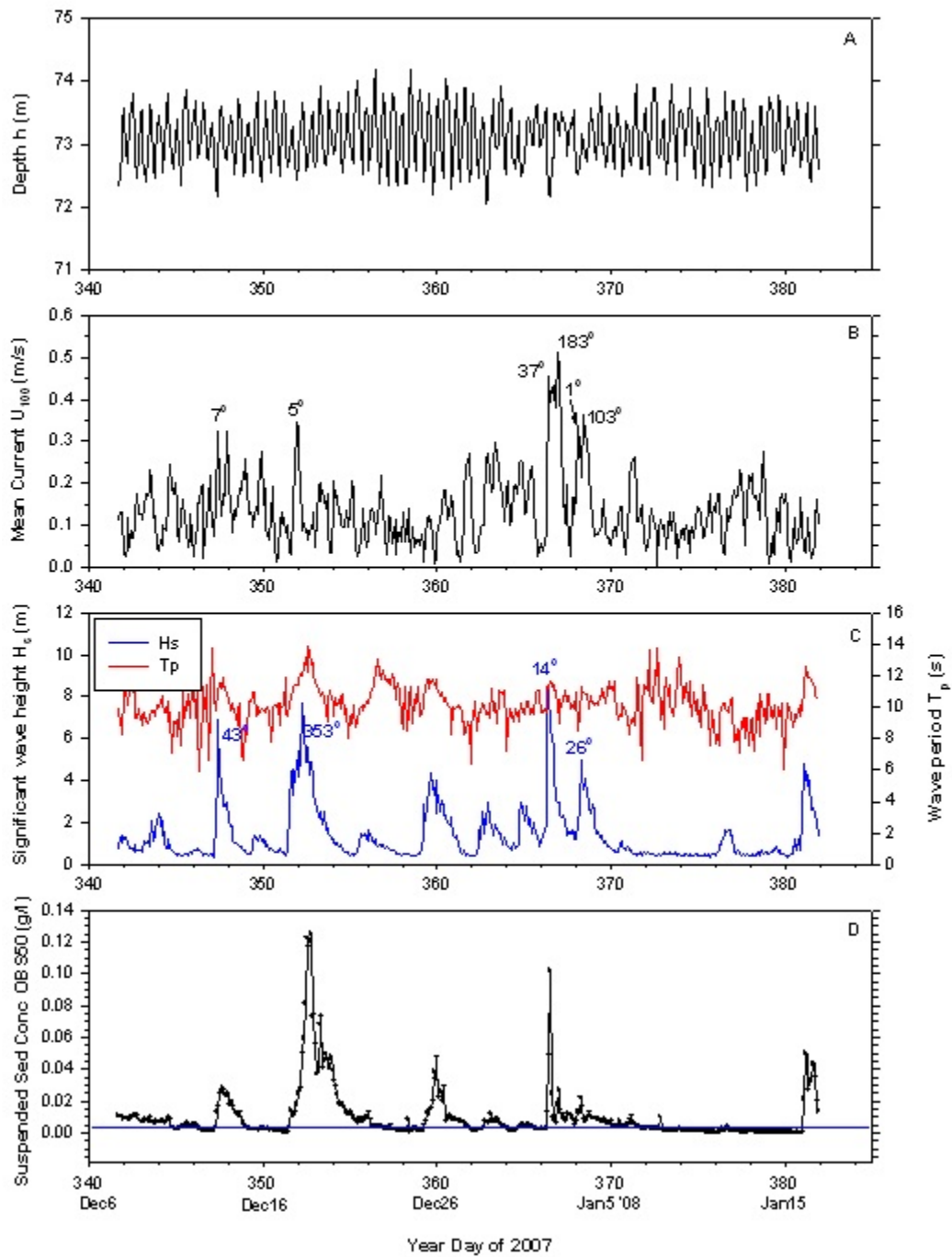


Figure 5 Time series plots of (a) mean water depth h , (b) mean current speed u_{100} , (c) significant wave height H_s , and wave period T_p , and (d) suspended sediment concentration at 50 cm above seabed OBS50 recorded by RALPH in the 2007 Green Bank deployment. Text labels in (b) and (c) indicate mean current and wave directions respectively. Blue line in (d) represents the estimated mean background suspended sediment concentration at ~ 5 mg/l.

value of 50-60 cm/s during the biggest storm recorded on yearday 367. This suggests that wind-driven flows during storms are the dominant component in the total near-bed currents on the Grand Banks. The strong near-bed mean currents during storms were dominantly to the N and NE, but could change to S and SSE during some storms (Figure 5b).

The suspended sediment concentration measured at 50 cm above the seabed (Fig. 5d) shows that sediment suspension occurred over several periods of time and that the maximum concentration reached approximately 120 mg/l. Comparison between Figs. 5b, 5c and 5d suggests that tidal current alone during fair-weather conditions is not strong enough to cause significant resuspension of the medium sand at the deployment site on Green Bank and that wave oscillatory flows and wind-driven currents during storms are responsible for the observed sediment resuspension events as these events were well correlated with the timing of the storms.

3.2 Relative impact of near-bed mean current and wave oscillation

Near-bed mean current U_{100} , significant wave orbital velocity u_b , and maximum instantaneous current speed u_m are compared in Figure 6 to assess the relative impact on the seabed by mean current and wave oscillatory flows. Moderate to strong mean currents of ~50 cm/s were observed, while maximum instantaneous current speed reached up to 120 cm/s. Near-bed significant wave orbital velocity reached 50-60 cm/s during this deployment. These are as strong as the mean current. Since the wave boundary layers are much thinner than that of mean current, the shear stress and impact on seabed sediment by waves during storms will be greater than the steady mean current on Green Bank.

3.3 Near-bed flows during storms

Figure 5 shows that the magnitude of the near-bed mean currents under fair-weather conditions, presumably mostly due to tidal current, was generally less than 25 cm/s. Mean currents during storms were much higher and reached 50-60 cm/s. The substantially higher near-bed mean currents during storms were due to wind-driven currents. Yearday (YD), significant wave height, wave propagation direction, mean current speed U_{100} and the direction of the mean current for the storms on yearday 366 and yearday 368 are listed in Tables 2 and 3, respectively. At the early stage of the storm on yearday 366, wave height quickly increased from 1 m to 7.6 m in 8 hours with a propagation direction (hence wind direction) to WNW shifting to N. Nearbed currents started to increase (from 8 cm/s to 14 cm/s) and the change of the current direction was similar to the wind and rotated from westward to northward. Wave height reached 8.5 m and wind was to NNE at the peak of the storm (day 366 hour 10). Nearbed mean current reached a peak value of 46 cm/s and was also to NE. As the storm waned (366:12 to 366:18), wave height was reduced to 4-6 m but wind direction remained to the NE. Nearbed mean current remained strong (> 40 cm/s) but its direction rotated from NE, to E, then to SE. As the storm continued the gradual degrading from 366:20 to 367:08, wave height decreased from 4 m to less than 2 m and the wind direction was steadily to the NNW. Nearbed current first decreased to 38 cm/s and then increased to another peak value of 51 cm/s before gradually decreasing to about 10 cm/s. In

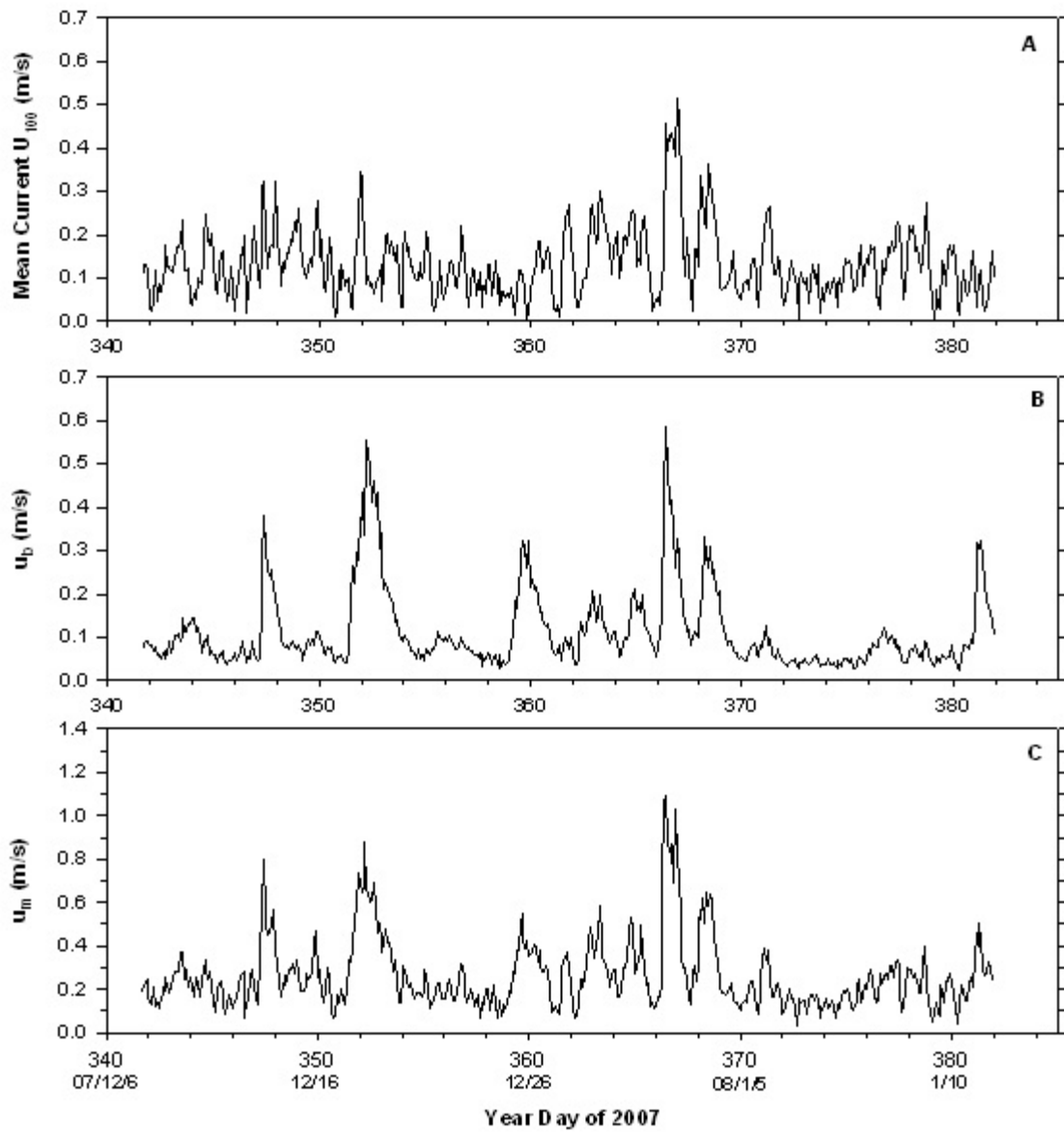


Figure 6 Time series plots of (a) near-bed mean current U_{100} , (b) significant wave orbital velocity u_b , and (c) maximum instantaneous current speed u_m measured during the 2007 Green Bank deployment.

Table 2 Yearday, hours, significant wave height, wave propagation direction, mean current speed U100 and mean current direction for the storm on yearday 366.

Day	Hour	Hs (m)	Wdir (degree)	U100 (m/s)	Cdir (degree)
366	0	1.04	290	0.057	306
366	2	1.391	281	0.038	255
366	4	1.542	280	0.06	257
366	6	1.892	355	0.083	263
366	8	7.627	6	0.143	4
366	10	8.501	14	0.457	37
366	12	6.3	20	0.394	57
366	14	6.224	36	0.429	77
366	16	5.413	19	0.432	110
366	18	4.327	15	0.41	141
366	20	3.043	3	0.38	153
366	22	2.986	0	0.512	183
367	0	2.983	348	0.471	198
367	2	2.417	355	0.467	235
367	4	2.239	344	0.303	258
367	6	2.302	348	0.179	276
367	8	2.134	349	0.104	325
367	10	1.36	339	0.195	20
367	12	1.688	341	0.121	51

Table 3 Yearday, hours, significant wave height, wave propagation direction, mean current speed U100 and mean current direction for the storm on yearday 368.

Day	Hour	Hs (m)	Wdir (degree)	U100 (m/s)	Cdir (degree)
368	0	1.175	294	0.177	332
368	2	1.94	323	0.336	1
368	4	2.71	359	0.293	8
368	6	4.987	26	0.232	21
368	8	4.142	18	0.215	62
368	10	3.556	25	0.361	103
368	12	4.055	21	0.321	122
368	14	3.358	353	0.297	168
368	16	2.974	337	0.249	189
368	18	2.682	329	0.221	218
368	20	2.415	324	0.171	228
368	22	2.892	325	0.109	245
369	0	2.581	319	0.082	208
369	2	1.96	313	0.072	245

contrast to the steady wind direction during this stage, the nearbed current continued to rotate from SE, through S, SW, to W and NW.

The nearbed current during the storm on yearday 368 demonstrated a similar process (see Table 3). It is speculated that this clockwise rotation of the nearbed current during storms is probably caused by the interaction between the rotation of tidal current and the wind-driven current process during storms.

4. SEDIMENT TRANSPORT AND SEABED STABILITY OBSERVATIONS

4.1 Bedforms

Imagenex sector scanning sonar fan-beam and pencil-beam images for yearday 366 hour 04 (366-04 hereafter) are compared in Figure 7 with associated wave height and current speed plotted beneath the sonar images. These images were recorded at the onset of the storm on yearday 366. The fan-beam image seems to show mostly homogenous seabed, however, the pencil-beam image (Figure 7b) does reveal mid-size wave ripples of approximately 20 cm wavelength. After 6-8 hours, the storm reached the peak condition of 8 m wave height and 0.5 m/s mean current (Figure 8). The fan-beam image recorded at the peak of the storm (Figure 8a) demonstrates that the seabed was possibly covered by large-wave ripples with ~2 m spacing. The pencil-beam image (Figure 8b) shows that the wave ripples of 20 cm wavelength recorded at yearday 366 hour 04 (Figure 7b) had been washed out by the storm and that mid-sized bedforms with 0.5 m spacing had developed.

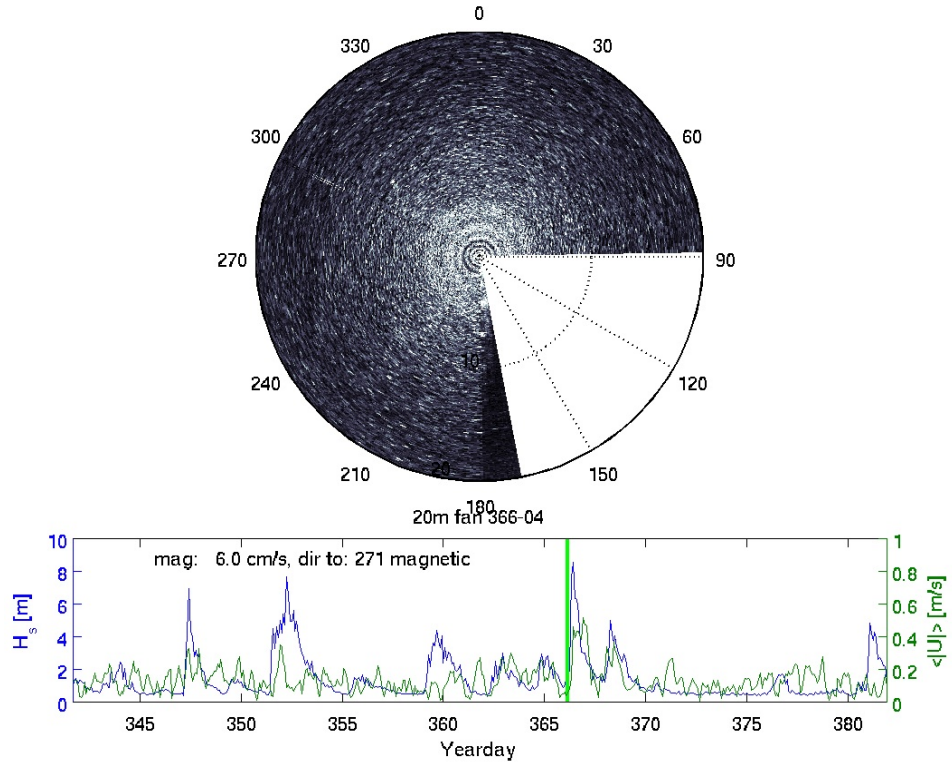
The fan-beam image recorded at yearday 352 hour 12 (Figure 9), immediately after the peak of the storm on yearday 352, shows the presence of a band of high backscatterance in the lower left quadrant. This could indicate the presence of coarse sediment in the trough of megaripples, although the absence of the feature in the subsequent burst (after only 2 hours) will contradict this interpretation.

4.2 Sediment suspension

Occurrence of sediment suspension was monitored with ABS and OBS sensors. The time series of the suspended sediment concentration (SSC) recorded by the six OBS sensors (Figure 10) demonstrate that several sediment suspension events occurred during this deployment and they are associated with the passing of the major storms over Green Bank. A maximum SSC of 200 mg/l was recorded at 13 cm above seabed. A weak trend of decreasing SSC with increasing distance above seabed can be detected. Nevertheless vertical advection of suspended sediment reached at least 1.1 m above the seabed during the major storms.

The seabed elevation change and suspended sediment concentration recorded by the ABS are shown in Figure 11. In agreement with the OBS data (Figure 10), the ABS data also demonstrates

A.



B.

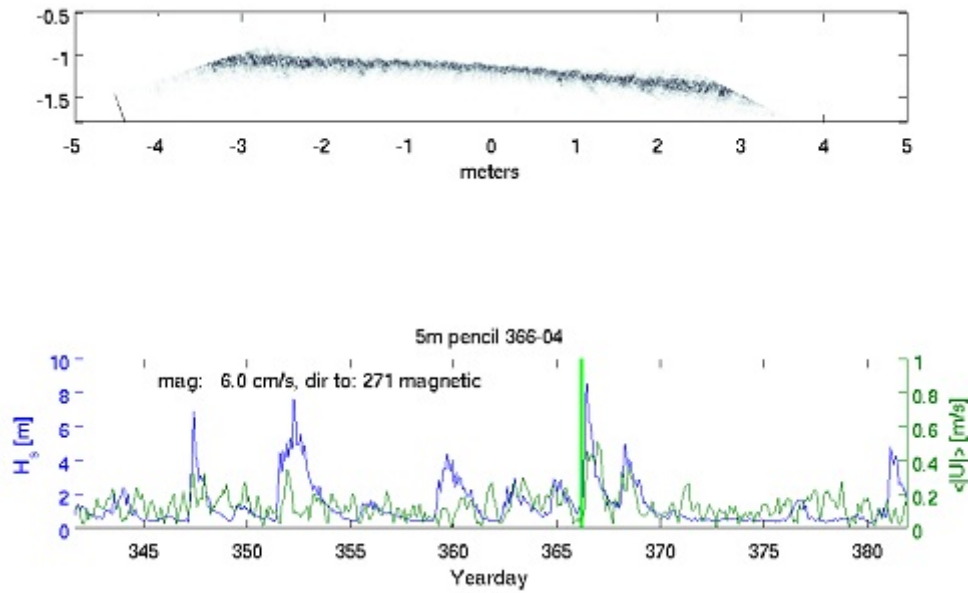
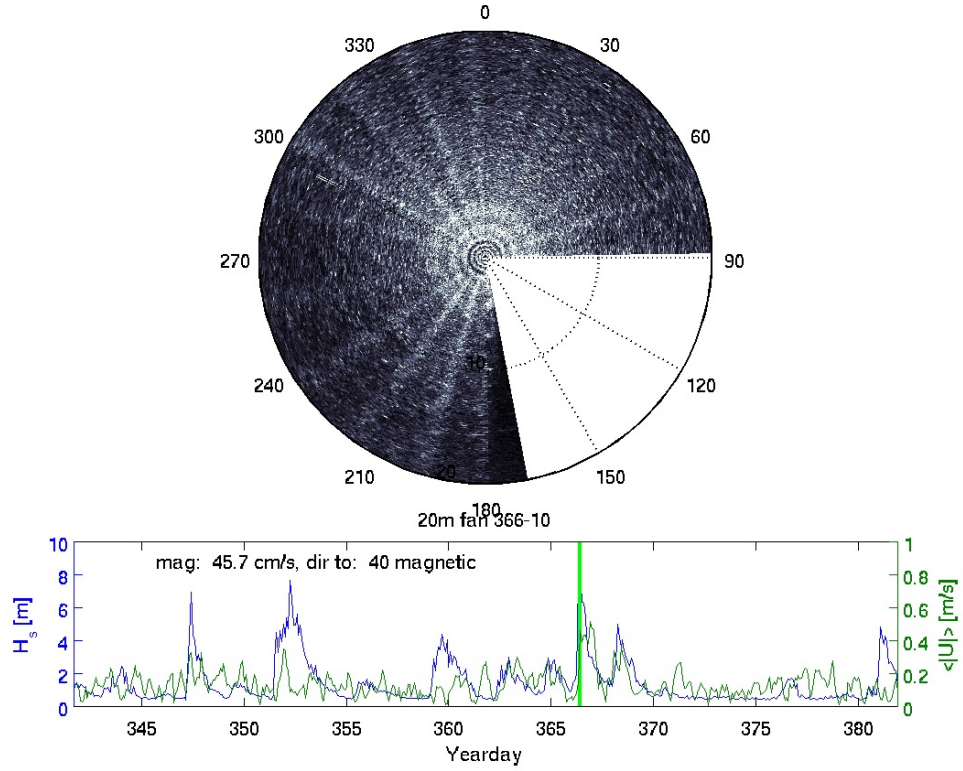


Figure 7 Imagenex sector scanning sonar fan-beam (a) and pencil-beam (b) images for yearday 366 hour 04 (366-04). The range of the fan-beam image is about 40 m and that of the pencil-beam image is about 6 m. The panels below the sonar images show the associated wave height (blue) and current speed (green) conditions.

A.



B.

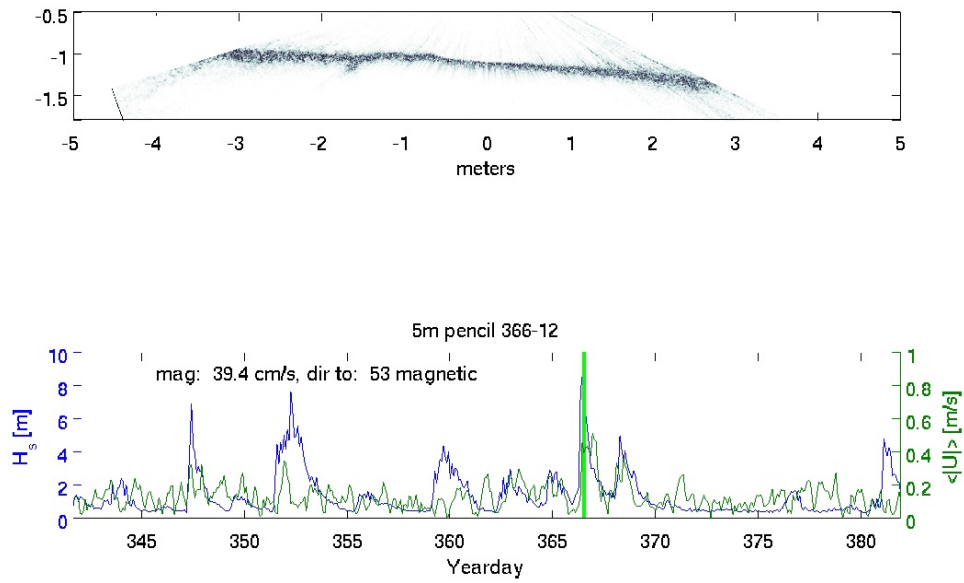


Figure 8 Imagenex sector scanning sonar fan-beam (a) and pencil-beam (b) images for yearday 366 hour 10 and yearday 366 hour 12 respectively, approximately at the peak of the storm. Other definitions are the same as that of Figure 7.

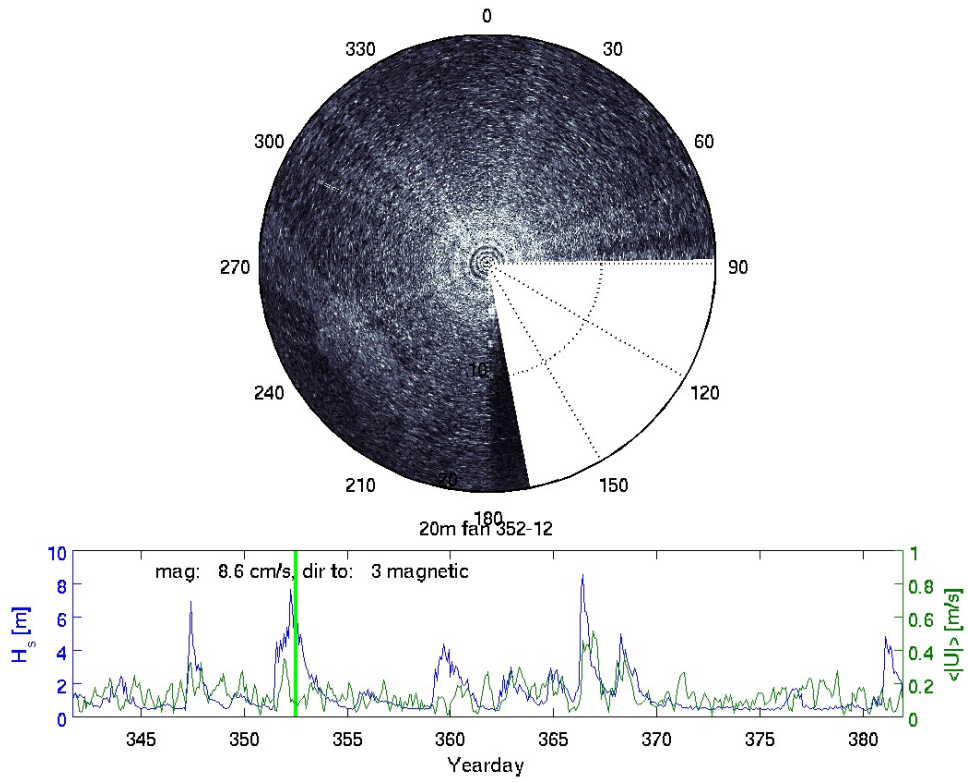


Figure 9 Imagenex sector scanning sonar fan-beam image for yearday 352 hour 12, immediately after the peak of the storm on yearday 352. Other definitions are the same as that of Figure 7.

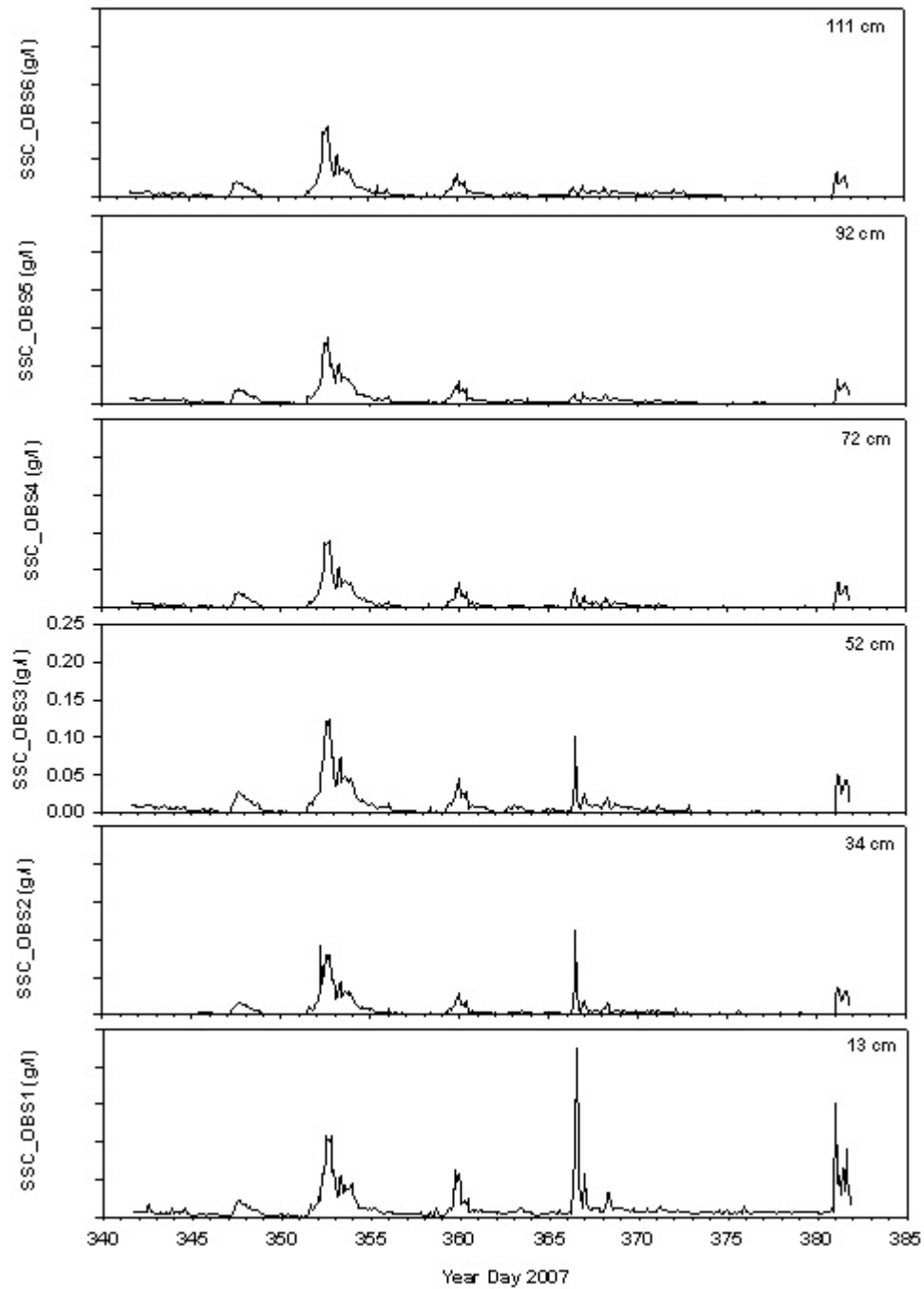


Figure 10 Time series plots of suspended sediment concentration (SSC) recorded by OBS sensors on RALPH in the 2007 Green Bank deployment. Numbers indicate the height of OBS above the seabed.

several suspension events in which the maximum SSC reached about 100 mg/l and suspended sediment reached up to 1 m above the seabed. The steps in the seabed elevation time series (boundary of the red near the bottom of the image) suggest that the seabed rose (alternatively the lander frame settled) several centimetres as storms passed on December 13th and 18th respectively.

Figure 12 compares the suspended sediment concentration burst data recorded by the ABS for 349-22 and 352-08 hours respectively. Burst 349-22 represents conditions under typical peak mean tidal current of 0.28 m/s with minimum wave effect (H_s at 1.1 m), and the ABS data show that tidal current alone does not cause sediment suspension (Fig. 12A). Burst 352-08 was at the peak of a storm with H_s of 6.5 m and weak mean current of 0.1 m/s (Fig. 12B). The ABS data from this burst show significant sediment resuspension and peak concentration of several 100s of mg/l close to the seabed. For bursts 351-18 and 351-22 (Fig. 13), wave conditions were similar. Values of H_s were 4.6 m and 5.0 m respectively. However, mean current was much stronger (0.35 m/s) for 351-22 than that for 351-18 (0.16 m/s). The associated ABS data show minimum sediment resuspension for 351-18 (e.g. 140-160 s) and more significant resuspension for 351-22. Suspended sediment concentration data from these two bursts demonstrate the importance of steady current and wave interaction in enhancing sediment resuspension on Green Bank.

The suspended sediment concentration recorded by the OBS at about 50 cm above the seabed (Fig. 5d) was averaged for the fairweather periods over the entire deployment duration. This provides an estimated mean background SSC of 5 mg/l (blue line in Fig. 5d). Comparison between the SSC data recorded by the OBS sensor with this background concentration suggests that some minimum level of sediment resuspension occurred in approximately 40% of time for the deployment duration. A more automated approach of comparing the OBS and ABS data with the low-pass filtered background values derived similar frequency of sediment resuspension, 33% of the time based on OBS data and over 37% of the time based on ABS data (Prescott, 2008).

5. PREDICTIONS BY SEDTRANS96

The application of the GSC sediment transport model SEDTRANS96 is an important aspect in studying bottom boundary layer dynamics and sediment transport on continental shelves (e.g., Amos, et al., 1996; Li et al., 1997). For given inputs of wave, current and seabed conditions, SEDTRANS96 applies the combined wave-current bottom boundary layer theory to predict wave-enhanced bed shear stresses, velocity profiles, suspended and bedload sediment transport rates and directions (Li and Amos, 2001). SEDTRANS96 requires several fluid and sediment parameters as inputs: mean grain size D , initial ripple height η and ripple wavelength λ , bed slope β , sediment density ρ_s and fluid density ρ . For the 2007 Green Bank data, the mean grain size D is 0.30 mm; ρ_s and ρ are taken as 2.65 and 1.025 g/cm³, respectively; and zero values are assumed for the initial ripple height, ripple wavelength, and bed slope. These values, together with the wave and current data in Appendix 1, were used in SEDTRANS96 (Li and Amos, 2001)

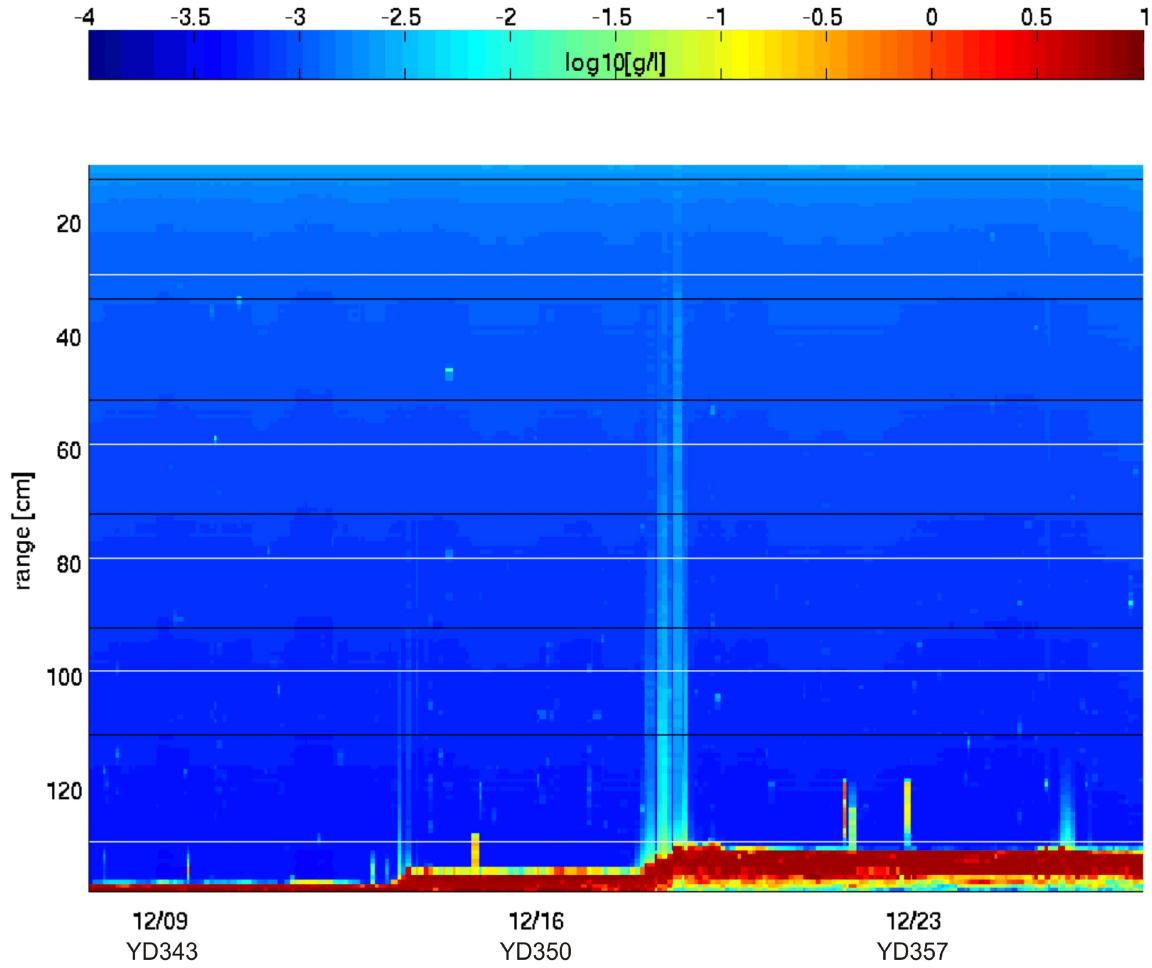


Figure 11 Seabed elevation and suspended sediment concentration profiles recorded by the ABS sensor. The y axis indicates the distance range away from the down-looking ABS mounted at 132 cm above the bottom. The color legend indicates \log_{10} of suspended sediment concentration (g/l) and the red boundary near the bottom shows seabed elevation change during the deployment duration.

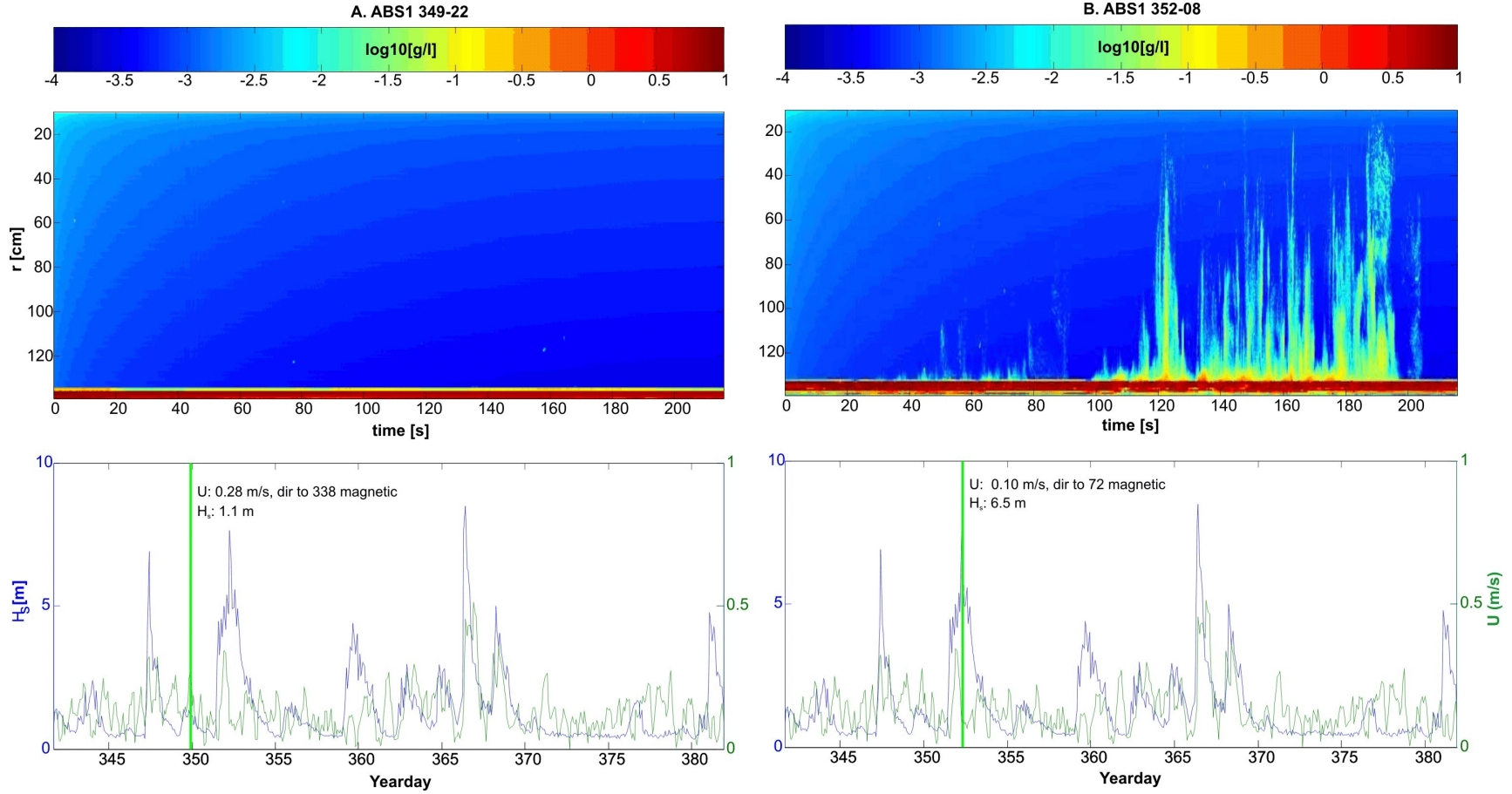


Figure 12 Suspended sediment concentration profiles recorded by the ABS sensor for (a) 349-22 and (b) 352-08. In the upper panels, r indicates the distance away from the ABS sensor towards the seabed and the color legend shows Log_{10} of suspended sediment concentration (g/l). The duration of the ABS data is about 220 seconds. The lower panels show the time series of significant wave height (H_s in blue) and mean current speed (U in green) for the entire deployment with the heavy vertical green line marking the time when the ABS burst was recorded.

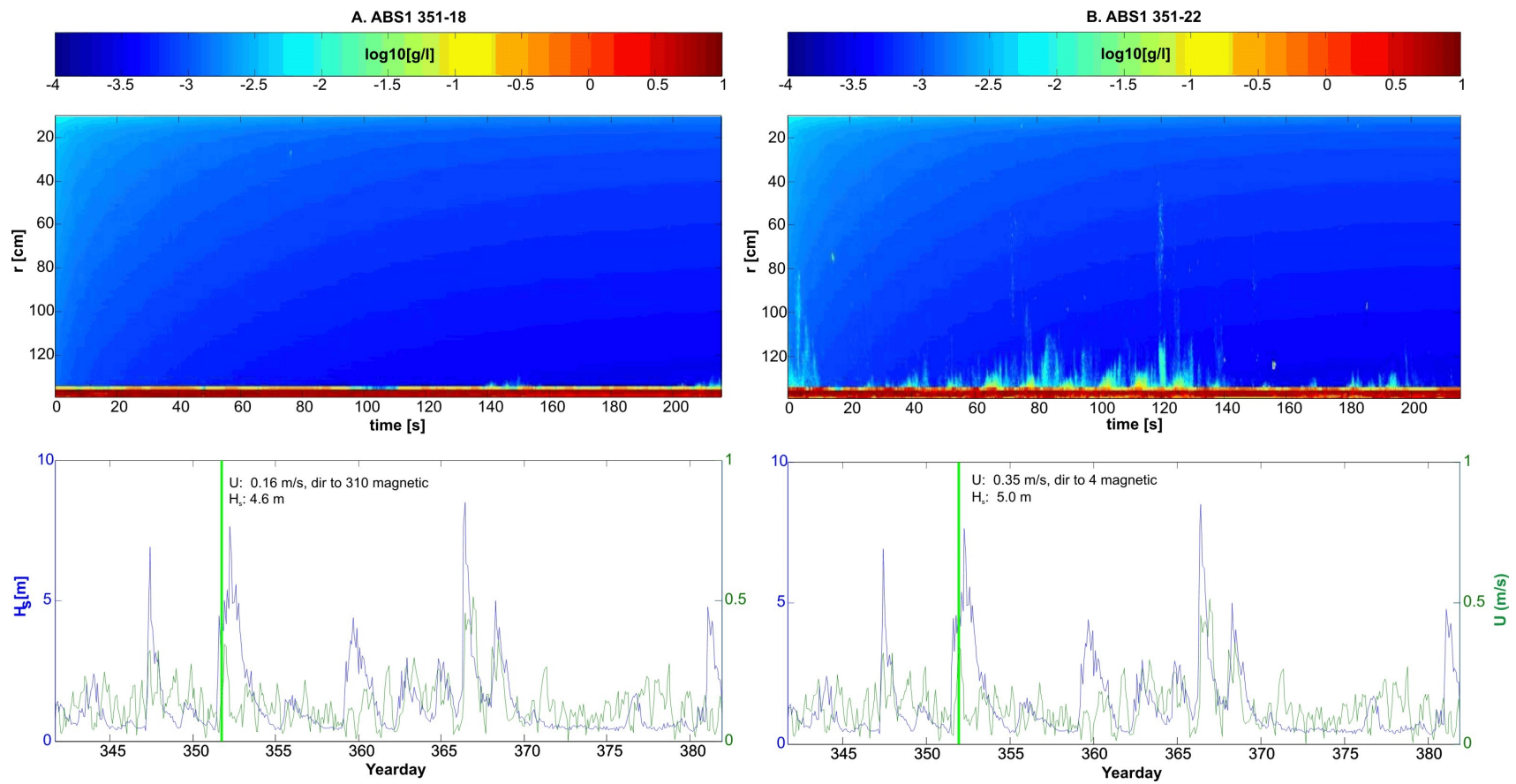


Figure 13 Suspended sediment concentration profiles recorded by the ABS sensor for (a) 351-18 and (b) 351-22. Definitions same as in Figure 12.

to predict various boundary layer dynamics and sediment transport parameters for the Green Bank 2007 deployment. The output of bottom boundary dynamics and sediment transport parameters from SEDTRANS96 are listed in Appendices 2 and 3 respectively.

Time series of model-predicted skin-friction (due to grain roughness only) current shear velocity u_{*cs} , wave shear velocity u_{*ws} , and combined wave-current shear velocity u_{*cws} are compared with the critical shear velocity for bedload transport, u_{*cr} , and the critical shear velocity for suspended load transport, u_{*crs} , in Figure 14. The values of u_{*cr} and u_{*crs} were computed according to Li and Amos (2001). Under non-storm conditions (periods of low u_{*ws} values; e.g., year day 342-347 and year day 372-380), the current shear velocity, presumably due to tidal currents, is generally less than 1.5 cm/s (Fig. 14a) and therefore not strong enough to transport the medium sand at the deployment site. During storms (indicated by the peaks of wave shear velocity in Fig. 14b; e.g., year day 352 and year day 367), the total current due to the addition of wind-driven currents to the tidal current is moderately higher than u_{*cr} of 1.45 cm/s, and can cause moderate bedload transport (Fig. 14a). More importantly, wave oscillations and wind-driven currents during these storms non-linearly interact to significantly enhance the near-bed forcing so that the combined-flow shear velocity increases up to 3.7 cm/s (Fig. 14c). The enhanced combined-flow shear velocities are not only substantially higher than u_{*cr} to cause significant bedload transport, but also exceed u_{*crs} in three events to cause suspended load transport in these storms (Fig. 14c).

The comparison between the model-predicted combined-flow shear velocity and the thresholds of bedload and suspended load transport in Fig. 14c suggests that bedload transport occurred for 12.2 % of the time and suspended load transport occurred for 1.7% of the time during the 2007 Green Bank deployment. These are quite lower than the frequencies estimated from comparing recorded OBS and ABS data with the background readings (section 4.2). The combined-flow shear velocity u_{*cws} in Fig. 14c is the spatially averaged skin-friction shear velocity. Previous studies have clearly demonstrated that when ripples are present, the shear velocity at the ripple crest is significantly enhanced from that averaged over the ripple length and that this ripple-enhanced shear should be used to determine the onset of sediment transport (e.g., Kapdasli and Dyer, 1986; Li et al., 1997). The discrepancy in estimating sediment transport frequencies could be due to the use of the spatially averaged shear velocity. Another explanation could be that the OBS and ABS sensors were seeing suspension of only the fine fractions of the sediment, which could be considerably finer than the 0.30 mm mean grain size used to derive the critical shear velocities for bedload and suspended load transport. Further discussion of the causes however is beyond the scope of this Open File report.

The mean grain size of 0.30 mm and the lander-recorded wave and current data were used in SEDTRANS96 to predict the bedload and suspended load transport rates and directions. Bedload transport rate was based on the Einstein-Brown (Brown, 1950) equation and the suspended load transport rate was derived from integrating the model-computed velocity and suspended sediment concentration profiles. The SEDTRANS96 model assumes that the advection of suspended sediment is due to the steady current. Thus the direction of suspended load transport is taken

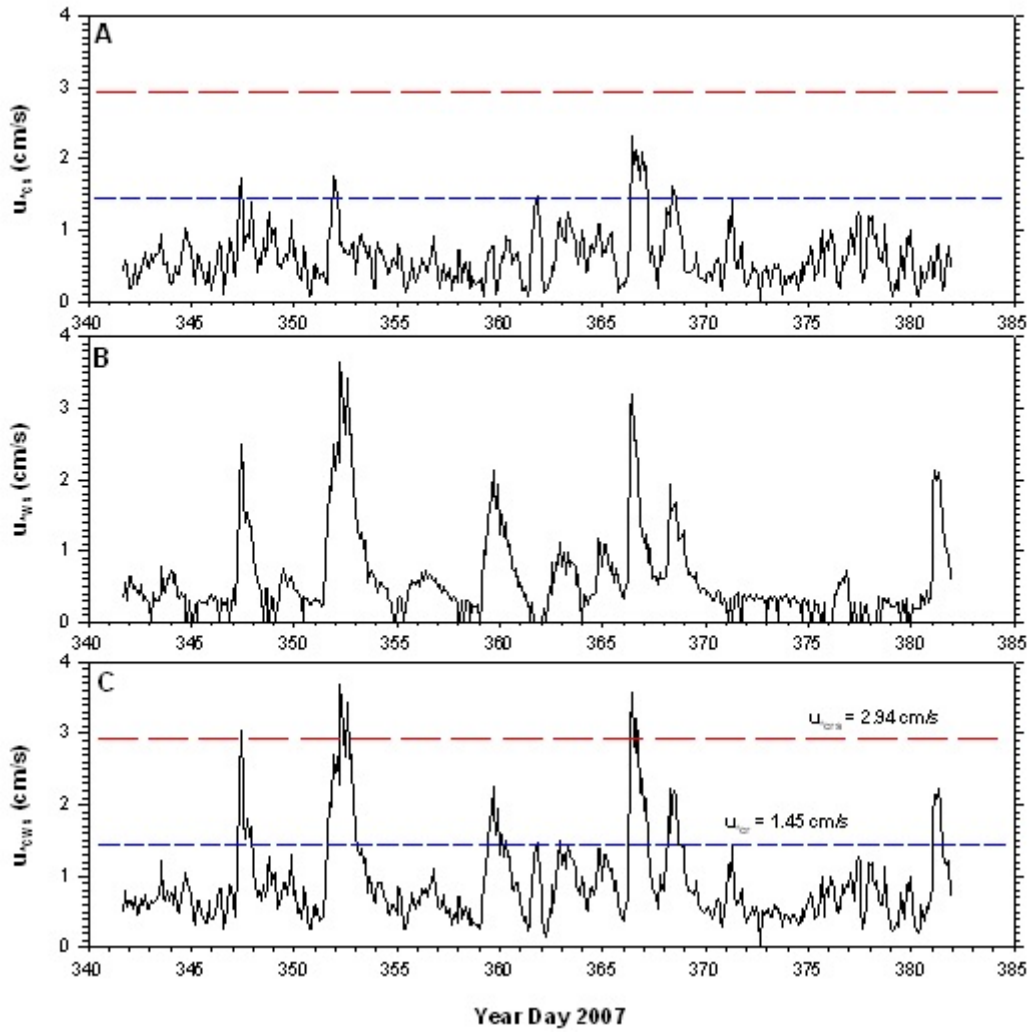


Figure 14 Time series of model-predicted skin-friction (a) current shear velocity u_{*cs} , (b) wave shear velocity u_{*ws} , and (c) combined wave-current shear velocity u_{*cws} , compared with the critical shear velocity for bedload transport u_{*cr} (blue short-dashed line) and the critical shear velocity for suspended load transport u_{*crs} (red long-dashed line).

as that of the mean current direction. The vector plots of the predicted bedload and suspended load transport flux (Fig. 15) demonstrate that infrequent (1.7% of the time), weak to moderate suspended load transport occur on Green Bank. The maximum value reaches 1.8 g/cm/s. Bedload transport is stronger and occurs more often (12.2% of the time). Peak bedload transport rates reach 5.7 g/cm/s. Sediment transport is dominantly to the northeast at the deployment site on Green Bank. A secondary direction to the SE is also observed. The dominant northeasterly sediment transport direction approximately conforms with the orientation of large bedforms in this area.

6. SUMMARY

The GSCA instrumented platform RALPH was deployed over a field of megaripples and sand waves in 71 m of water depth on Green Bank, western Grand Banks, in the winter of 2007 to collect in situ sediment dynamics data for improved understanding of nearbed wave and current forcing and sediment and bedform mobility at this site. Key sensors on RALPH were programmed to burst sample for a 15 minute duration every 2 hours at a frequency of 2 Hz. Most sensors worked well during this deployment. On the whole, the hydrodynamic data were of better quality than any previous lander deployment. This was the maiden deployment for the newly acquired Nobska MAVS 3D acoustic current meter. There were no problems at all with this instrument. This current meter system can sample 5 times faster than the ALEC EMCs, has enough memory for a longer burst length and also longer deployment duration, and provides the important addition of the vertical velocity component. The 3-component velocity measurement allows for Reynold's stress and inertial dissipation estimates of bed shear stress.

The hydrodynamics data clearly demonstrate the dominance of the semi-diurnal tides on Green Bank with a maximum tidal range of about 2 m. Several storms were recorded during this deployment. The significant wave heights and wave periods in these storms ranged 3-8.5 m and 8-14 s respectively. The magnitude of the near-bed mean currents under fair-weather conditions, presumably mostly due to tidal current, was generally less than 25 cm/s. But the speed of near-bed mean currents was increased to 50-60 cm/s during the major storms recorded. The maximum near-bed instantaneous current speed reached up to 120 cm/s and half of this was contributed from wave oscillatory flows as the near-bed significant wave orbital velocity reached 50-60 cm/s during major storms. This suggests that near-bed wave oscillation and steady wind-driven currents during storms significantly affect the seabed shear stress and sediment transport on Green Bank.

Active bedforms were observed during this deployment. These include mid-size wave ripples of approximately 20 cm wavelength at the onset of storms, and large-wave ripples with ~2 m spacing at or immediately after the peaks of storms. Sediment sensors on the lander recorded several sediment resuspension events in which maximum suspended sediment concentration (SSC) reached nearly 200 mg/l at 13 cm above the seabed. Comparison between the timing of the

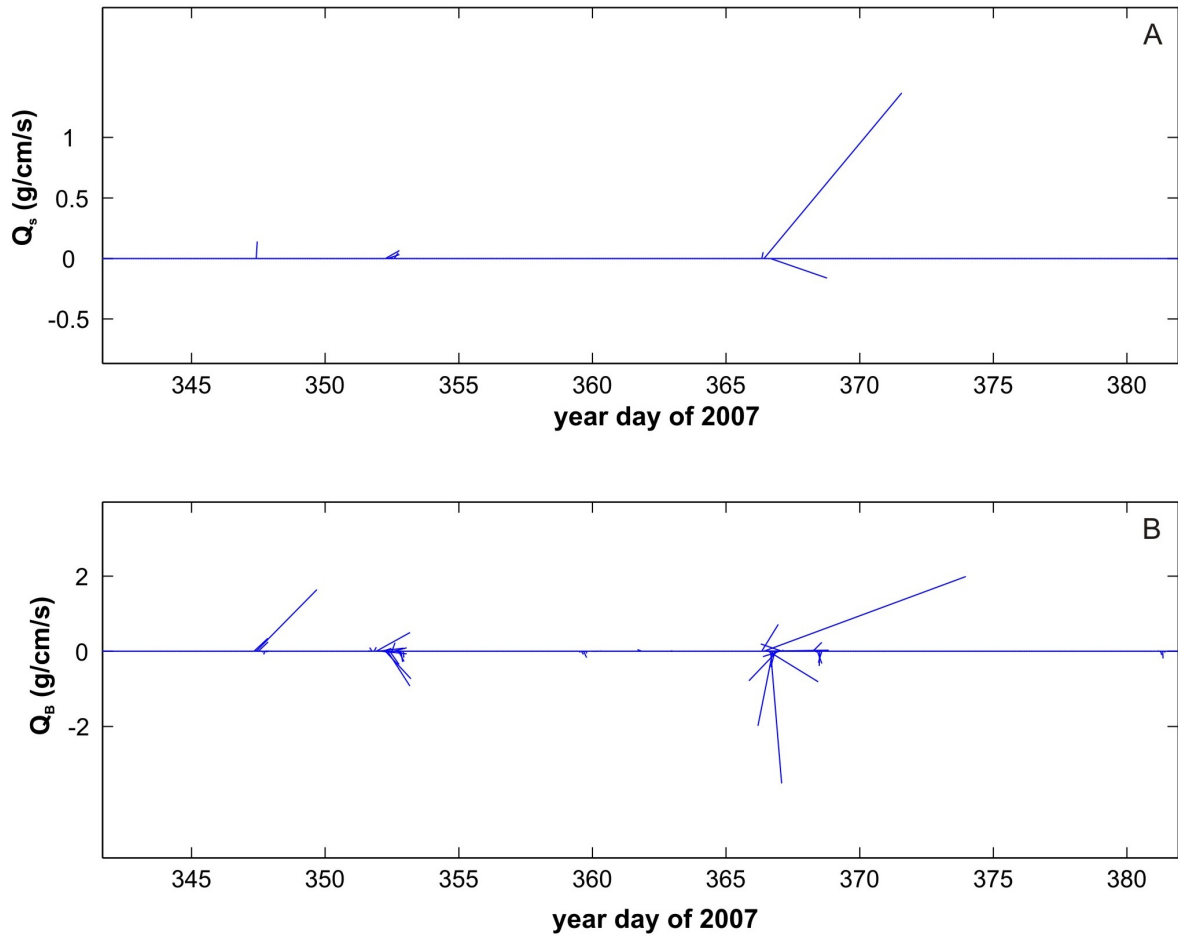


Figure 15 Vector plots of suspended load (a) and bedload (b) transport fluxes calculated from SEDTRANS96 model, based on the mean grain size of 0.30 mm and lander-recorded wave and current parameters.

observed resuspension events and the recorded wave and current parameters suggests that tidal current alone during fair-weather conditions is not strong enough to cause sediment resuspension at the deployment site on Green Bank and that wave oscillatory flows and wind-driven currents during storms are responsible for the observed sediment resuspension events as these events were well correlated with the timing of the storms. Instantaneous suspended sediment concentration data recorded by the ABS sensor further indicate that the maximum instantaneous suspended sediment concentration reached several 100s of mg/l close to the seabed. Assessment of suspended sediment concentration data recorded by the ABS sensor under different wave and steady current conditions also shows that under similar wave conditions, the presence of strong mean-current enhances sediment resuspension on Green Bank. Comparison between the SSC data recorded by the OBS sensor with the background concentration suggests that minimum level of sediment resuspension occurred in approximately 40% of time for the deployment duration.

The wave, current and sediment data obtained from the 2007 Green Bank deployment were used as inputs to the continental shelf sediment transport model SEDTRANS96 to predict various boundary layer dynamics and sediment transport parameters. The model-predicted shear velocity data show that under non-storm conditions, the tidal current shear velocity is generally less than 1.5 cm/s and is not strong enough to cause transport of the medium sand at the deployment site. When storms pass this area, the addition of wind-driven currents to the tidal current causes the current shear velocity to be moderately higher than 1.5 cm/s. The interaction between waves and the enhanced steady current further produces combined-flow shear velocities up to 3.7 cm/s to cause not only significant bedload transport, but also periodic events of suspended load transport. The predicted bedload and suspended load transport rates indicate that bedload transport is dominant over the suspended load during the 2007 deployment. Peak bedload transport rate reaches 5.7 g/cm/s during storms and the direction is dominantly to the northeast at the deployment site on Green Bank.

ACKNOWLEDGEMENT

The authors would like to thank Edward King for providing the background geological information that helped the selection of the deployment site; Bruce Wile and David Morse for co-ordinating field support and logistics of opportune CCG ships; and Bob Murphy and Murray Scotney (DFO) for technical support in the deployment and retrieval of the lander. The support of the captain and crew of CCGS Hudson was greatly appreciated. Finally, this report benefited from the critical review by E. King. This project was jointly funded by Earth Science Sectors Offshore Geoscience Program, and the Program of Energy Research and Development (PERD) through the Nearbed Wave and Current Forcing and Sediment Dynamics project (B15.003).

REFERENCES

- Amos, C.L., Li, M.Z. and Choung, K-S., 1996. Storm-generated, hummocky stratification on the outer-Scotian Shelf. *Geo-Marine Letters*, 16: 85-94.
- Brown, C.B., 1950. In: H. Rouse, (ed.), *Engineering Hydraulics*, John Wiley and Sons, New York, 1039pp.
- Heffler, D.E., 1996. RALPH - A dynamic instrument for sediment dynamics. *Proc. Oceans'96, IEEE, Ft. Lauderdale, Florida, USA, September 1996*, p. 728-732.
- Kapdasli, M.S. and Dyer, K.R., 1986. Threshold conditions for sand movement on a rippled bed. *Geo-Marine Letters*, 6: 161-164.
- King, E.L., 2002. Sable Island Bank shallow geological conditions: Geohazard atlas and catalogue compiled from shallow reflection seismic data. Unpublished Final report to Sable Offshore Energy Incorporated by the Geological Survey of Canada. December 2002.
- Li, M.Z. and Amos, C.L., 1999. Sheet flow and large wave ripples under combined waves and currents: Their field observation, model prediction and effects on boundary layer dynamics. *Cont. Shelf Res.*, 19: 637-663.
- Li, M.Z. and Amos, C.L., 2001. SEDTRANS96: The Upgraded and Better Calibrated Sediment-Transport Model for Continental Shelves. *Computers and Geosciences*, 27: 619-645.
- Li, M.Z. and King, E.L., 2007. Multibeam bathymetric investigations of the morphology of sand ridges and associated bedforms and their relation to storm processes, Sable Island Bank, Scotian Shelf. *Mar. Geol.*, 243: 200-228. doi:10.1016/j.margeo.2007.05.004
- Li, M.Z., Amos, C.L., Zevenhuizen, J., Heffler, D.E., Wile, B., and Drapeau, G., 1994. Hydrodynamics and Seabed Stability Observations on Sable Island Bank - AGC/LASMO Joint Program: A Summary of the Data for 1993/94. Geological Survey of Canada Open File Report 2949.
- Li, M.Z., Amos, C.L. and Heffler, D.E., 1997. Boundary layer dynamics and sediment transport under storm and non-storm conditions on the Scotian shelf. *Marine Geology*, 141: 157-181.
- Li, M.Z., Amos, C.L., and Heffler, D.E., 1999. Hydrodynamics and Seabed Stability Observations on Sable Island Bank: A Summary of the Data for 1996/97. Geological Survey of Canada Open File Report 2997.

Li, M.Z., King, E.L. And Smyth, C., 2003. Morphology and Stability of Sand Ridges on Sable Island Bank, Scotian Shelf. GSCA Open File 1836, 52 pp.

Li, M. Z., King, E.L. and Prescott, R.H., in press. Seabed disturbance and bedform distribution and mobility on the storm dominated Sable Island Bank, Scotian Shelf. In: Sediments, Morphology and Sedimentary Processes on Continental Shelves, Li, M.Z., Sherwood, C. and Hill, P. (Eds.), Special Publication of International Association of Sedimentologists, Blackwell Science, Berlin.

Prescott, R., 2008. Summary of 2007 Green Bank Ralph Deployment. Contract Report, Prescott and Zou Consulting.

Smyth, C., Li, M.Z. and Heffler, D.E., 2003. A summary of the 2001 Sable Island Bank hydrodynamic and bedform data. GSC Open File Report 1788.

Appendix 1: Burst-averaged wave, current and sediment suspension parameters for the 2007 Green Bank deployment. Depth is in meter; U100 is the mean velocity at 100 cm above seabed (in m/s); Cdir is the mean current (flow toward) direction (magnetic north degree), Hs is the significant wave height (in m), Tp is wave period (in second) from velocity spectral analysis, Wdir is the wave propagation (toward) direction (magnetic north degree) and OBS50 is the suspended sediment concentration measured at 50 cm above seabed.

Day	Hour	YearDay	Depth	U100	Cdir	Hs	Tp	Wdir	OBS50
341	16	341.67	72.33	0.113	211	0.79	9.94	325	0.0110
341	18	341.75	72.50	0.129	259	1.33	8.89	336	0.0104
341	20	341.83	72.93	0.129	260	1.40	9.31	312	0.0103
341	22	341.92	73.35	0.123	273	1.04	8.24	321	0.0095
342	0	342.00	73.56	0.031	259	1.30	10.84	326	0.0086
342	2	342.08	72.81	0.026	260	1.26	11.31	328	0.0090
342	4	342.17	72.78	0.047	266	1.15	10.17	325	0.0090
342	6	342.25	72.70	0.118	326	1.07	10.25	334	0.0088
342	8	342.33	73.43	0.048	320	0.80	10.94	331	0.0089
342	10	342.42	73.55	0.085	246	0.80	11.18	321	0.0098
342	12	342.50	73.80	0.070	230	0.70	11.00	316	0.0104
342	14	342.58	73.02	0.095	222	0.92	11.14	313	0.0106
342	16	342.67	72.79	0.127	280	0.57	9.36	297	0.0108
342	18	342.75	72.45	0.177	335	0.65	9.30	299	0.0106
342	20	342.83	72.82	0.126	17	0.63	9.91	320	0.0093
342	22	342.92	73.50	0.126	72	0.63	9.20	325	0.0081
343	0	343.00	73.54	0.120	74	0.55	9.50	322	0.0068
343	2	343.08	72.78	0.115	64	0.70	8.88	327	0.0072
343	4	343.17	72.62	0.139	43	1.11	9.63	339	0.0070
343	6	343.25	72.40	0.173	39	1.00	9.06	356	0.0090
343	8	343.33	72.83	0.172	45	1.14	8.97	346	0.0079
343	10	343.42	73.41	0.180	76	0.88	9.36	6	0.0072
343	12	343.50	73.63	0.232	107	0.88	9.40	22	0.0099
343	14	343.58	73.49	0.210	151	2.05	9.81	21	0.0075
343	16	343.67	72.62	0.118	184	1.13	9.76	17	0.0067
343	18	343.75	72.46	0.120	206	1.34	9.47	43	0.0058
343	20	343.83	72.74	0.123	247	1.82	9.54	56	0.0073
343	22	343.92	73.22	0.045	248	1.88	10.18	55	0.0069
344	0	344.00	73.46	0.038	209	2.40	9.98	62	0.0070
344	2	344.08	73.12	0.064	140	2.24	10.39	63	0.0070
344	4	344.17	72.92	0.050	151	1.38	10.70	70	0.0074
344	6	344.25	72.56	0.102	214	2.04	10.21	65	0.0075
344	8	344.33	72.93	0.090	270	1.09	9.70	78	0.0065
344	10	344.42	73.51	0.088	220	0.79	9.65	51	0.0067
344	12	344.50	73.79	0.151	220	0.76	10.34	68	0.0076
344	14	344.58	73.52	0.187	215	1.17	9.07	55	0.0096
344	16	344.67	73.14	0.245	228	0.80	9.63	64	0.0084
344	18	344.75	72.76	0.187	265	0.65	7.14	67	0.0034
344	20	344.83	72.62	0.174	286	0.56	9.09	44	0.0032
344	22	344.92	73.08	0.201	335	0.54	8.96	316	0.0024
345	0	345.00	73.39	0.144	357	0.43	9.24	311	0.0021
345	2	345.08	73.19	0.082	50	0.52	8.10	298	0.0023
345	4	345.17	72.96	0.063	134	0.51	9.64	281	0.0035
345	6	345.25	72.34	0.122	274	0.45	7.58	295	0.0028
345	8	345.33	72.94	0.158	323	0.42	9.72	258	0.0033
345	10	345.42	73.49	0.163	307	0.41	10.95	238	0.0047
345	12	345.50	73.62	0.116	3	0.49	9.37	323	0.0044
345	14	345.58	73.85	0.089	90	0.47	10.03	7	0.0049
345	16	345.67	73.25	0.048	189	0.42	10.85	18	0.0060
345	18	345.75	72.75	0.065	266	0.54	9.35	16	0.0047
345	20	345.83	72.81	0.126	296	0.56	10.09	331	0.0044
345	22	345.92	73.29	0.080	289	0.51	10.59	284	0.0041
346	0	346.00	73.41	0.026	334	0.69	11.31	300	0.0037
346	2	346.08	73.68	0.084	175	0.69	9.35	311	0.0055
346	4	346.17	72.92	0.088	194	0.65	11.60	313	0.0052
346	6	346.25	72.78	0.155	248	0.74	8.66	326	0.0042
346	8	346.33	72.86	0.153	269	0.68	5.89	294	0.0029
346	10	346.42	73.11	0.194	290	0.63	8.75	310	0.0023
346	12	346.50	73.62	0.198	308	0.51	9.34	303	0.0013
346	14	346.58	73.66	0.021	246	0.45	11.30	307	0.0012
346	16	346.67	73.49	0.080	191	0.46	9.86	264	0.0018
346	18	346.75	72.81	0.103	238	0.47	11.39	275	0.0014
346	20	346.83	72.74	0.156	271	0.45	6.57	248	0.0014
346	22	346.92	73.11	0.218	300	0.46	9.84	252	0.0011
347	0	347.00	73.18	0.152	335	0.49	10.11	226	0.0013
347	2	347.08	73.33	0.115	354	0.54	13.76	262	0.0009
347	4	347.17	72.92	0.076	7	0.36	10.65	229	0.0010
347	6	347.25	72.33	0.157	353	2.09	9.76	48	0.0034
347	8	347.33	72.16	0.310	357	4.19	11.12	58	0.0132
347	10	347.42	72.55	0.323	7	6.91	10.88	43	0.0161
347	12	347.50	73.48	0.199	24	4.30	11.58	34	0.0245
347	14	347.58	73.59	0.124	77	3.96	11.19	39	0.0265
347	16	347.67	73.32	0.171	126	2.75	11.93	53	0.0289
347	18	347.75	73.06	0.174	163	3.14	11.27	24	0.0263
347	20	347.83	72.82	0.171	203	2.80	11.28	15	0.0228
347	22	347.92	72.76	0.323	232	2.94	10.77	23	0.0244
348	0	348.00	73.19	0.213	241	2.15	10.65	16	0.0238
348	2	348.08	73.46	0.132	274	1.83	9.73	11	0.0179
348	4	348.17	73.33	0.125	258	1.79	9.94	21	0.0194
348	6	348.25	73.18	0.081	311	1.09	10.22	12	0.0159
348	8	348.33	72.52	0.136	290	1.01	9.80	358	0.0151

Day	Hour	YearDay	Depth	U100	Cdir	Hs	Tp	Wdir	OBS50
348	10	348.42	72.81	0.123	279	1.05	9.52	14	0.0129
348	12	348.50	73.32	0.159	258	0.97	8.89	354	0.0118
348	14	348.58	73.72	0.157	237	0.97	9.79	0	0.0110
348	16	348.67	73.57	0.187	233	0.83	10.29	348	0.0128
348	18	348.75	73.25	0.185	259	0.88	7.12	336	0.0105
348	20	348.83	72.50	0.229	281	0.69	6.68	310	0.0064
348	22	348.92	72.58	0.208	308	0.67	8.89	307	0.0052
349	0	349.00	72.93	0.259	330	0.55	8.81	314	0.0038
349	2	349.08	73.32	0.195	333	0.47	8.23	343	0.0028
349	4	349.17	73.34	0.127	354	0.47	10.39	281	0.0029
349	6	349.25	72.94	0.133	12	0.50	10.31	267	0.0026
349	8	349.33	72.56	0.116	323	0.67	10.76	313	0.0023
349	10	349.42	72.62	0.098	331	1.03	10.99	316	0.0024
349	12	349.50	73.31	0.122	300	1.37	11.00	311	0.0024
349	14	349.58	73.47	0.146	286	1.26	9.45	311	0.0021
349	16	349.67	73.84	0.127	278	1.12	9.56	314	0.0020
349	18	349.75	73.09	0.169	298	1.12	9.96	328	0.0012
349	20	349.83	72.54	0.246	334	1.34	9.66	348	0.0031
349	22	349.92	72.39	0.276	336	1.12	9.92	346	0.0030
350	0	350.00	73.04	0.149	13	1.17	9.81	346	0.0028
350	2	350.08	73.44	0.189	19	0.85	9.68	324	0.0026
350	4	350.17	73.68	0.089	40	1.14	9.84	350	0.0021
350	6	350.25	73.15	0.081	131	0.90	9.96	349	0.0024
350	8	350.33	72.98	0.067	189	0.70	9.81	355	0.0029
350	10	350.42	72.55	0.118	265	0.75	7.77	344	0.0018
350	12	350.50	73.10	0.194	291	0.71	8.91	332	0.0021
350	14	350.58	73.24	0.158	318	0.63	9.86	2	0.0014
350	16	350.67	73.83	0.057	357	0.62	10.14	354	0.0018
350	18	350.75	73.57	0.011	160	0.57	10.01	332	0.0013
350	20	350.83	72.80	0.025	251	0.58	10.19	338	0.0018
350	22	350.92	72.50	0.116	253	0.72	8.90	317	0.0013
351	0	351.00	72.66	0.073	272	0.69	10.22	322	0.0017
351	2	351.08	73.29	0.132	311	0.59	10.04	314	0.0009
351	4	351.17	73.68	0.114	281	0.56	10.12	320	0.0007
351	6	351.25	73.31	0.083	294	0.40	11.93	262	0.0007
351	8	351.33	72.92	0.096	346	0.41	9.57	296	0.0006
351	10	351.42	72.65	0.102	341	0.69	9.42	281	0.0006
351	12	351.50	72.76	0.036	340	2.73	10.08	278	0.0030
351	14	351.58	73.18	0.029	218	4.46	10.72	273	0.0144
351	16	351.67	73.29	0.136	238	3.27	11.12	273	0.0129
351	18	351.75	73.08	0.163	312	4.56	11.21	295	0.0105
351	20	351.83	72.75	0.222	355	3.93	11.39	314	0.0134
351	22	351.92	72.44	0.346	5	5.00	11.47	312	0.0180
352	0	352.00	72.69	0.336	19	4.18	11.38	315	0.0240
352	2	352.08	73.00	0.246	23	5.38	11.66	323	0.0260
352	4	352.17	73.09	0.214	22	4.70	12.10	340	0.0285
352	6	352.25	73.66	0.088	53	7.65	11.99	353	0.0504
352	8	352.33	73.40	0.103	74	6.51	12.60	350	0.0595
352	10	352.42	72.58	0.082	75	4.90	13.17	346	0.0811
352	12	352.50	72.77	0.086	358	4.92	12.23	351	0.1221
352	14	352.58	72.65	0.065	33	5.56	13.93	354	0.1170
352	16	352.67	73.08	0.083	42	4.30	13.64	357	0.1208
352	18	352.75	73.40	0.098	71	4.92	12.71	358	0.1251
352	20	352.83	73.51	0.106	112	4.09	12.85	8	0.0733
352	22	352.92	72.79	0.132	118	3.43	12.06	1	0.0738
353	0	353.00	72.65	0.048	172	2.95	11.72	359	0.0557
353	2	353.08	72.76	0.118	205	2.70	11.34	357	0.0368
353	4	353.17	73.52	0.193	212	2.25	11.22	357	0.0378
353	6	353.25	73.92	0.203	212	2.55	10.77	353	0.0681
353	8	353.33	73.83	0.158	200	2.33	10.85	349	0.0732
353	10	353.42	73.11	0.183	205	1.91	10.94	354	0.0411
353	12	353.50	72.71	0.161	225	2.49	10.63	357	0.0459
353	14	353.58	72.67	0.138	258	1.61	9.77	10	0.0494
353	16	353.67	72.97	0.175	265	1.73	9.04	351	0.0468
353	18	353.75	73.70	0.092	309	1.47	10.48	4	0.0456
353	20	353.83	73.46	0.033	248	1.33	11.04	360	0.0409
353	22	353.92	73.06	0.034	173	1.31	10.63	4	0.0476
354	0	354.00	72.91	0.153	236	1.06	10.40	359	0.0393
354	2	354.08	72.85	0.207	274	1.17	9.42	1	0.0330
354	4	354.17	72.90	0.164	308	0.94	10.58	339	0.0295
354	6	354.25	73.42	0.171	305	1.00	10.18	349	0.0240
354	8	354.33	73.66	0.126	328	0.84	10.47	352	0.0182
354	10	354.42	73.34	0.127	354	0.93	9.94	337	0.0172
354	12	354.50	72.84	0.101	341	0.90	10.69	339	0.0183
354	14	354.58	72.56	0.094	335	0.64	10.87	326	0.0160
354	16	354.67	73.00	0.095	199	0.60	9.54	314	0.0164
354	18	354.75	73.13	0.137	247	0.59	9.91	253	0.0141
354	20	354.83	73.83	0.110	257	0.59	8.31	298	0.0121
354	22	354.92	73.30	0.098	256	0.51	8.07	250	0.0122
355	0	355.00	73.07	0.120	281	0.41	9.45	241	0.0119
355	2	355.08	72.80	0.205	324	0.48	8.99	237	0.0134

Day	Hour	YearDay	Depth	U100	Cdir	Hs	Tp	Wdir	OBS50
355	4	355.17	72.70	0.186	326	0.48	10.17	232	0.0099
355	6	355.25	73.27	0.136	329	0.41	9.91	221	0.0088
355	8	355.33	73.73	0.052	293	0.48	8.76	209	0.0078
355	10	355.42	74.02	0.026	35	0.63	9.11	223	0.0062
355	12	355.50	73.55	0.039	224	0.92	9.75	244	0.0093
355	14	355.58	72.97	0.069	268	1.47	10.02	256	0.0091
355	16	355.67	72.53	0.113	303	1.38	10.17	248	0.0073
355	18	355.75	72.95	0.139	316	1.37	9.77	245	0.0072
355	20	355.83	73.45	0.079	312	1.48	9.97	237	0.0082
355	22	355.92	73.56	0.049	263	1.24	10.26	234	0.0094
356	0	356.00	73.40	0.071	305	1.64	10.43	228	0.0097
356	2	356.08	72.59	0.086	301	1.10	10.30	235	0.0127
356	4	356.17	72.88	0.129	287	1.50	10.79	240	0.0079
356	6	356.25	73.01	0.140	290	1.25	11.21	248	0.0044
356	8	356.33	73.89	0.125	320	1.00	11.28	237	0.0045
356	10	356.42	74.18	0.085	301	1.17	12.62	227	0.0045
356	12	356.50	73.47	0.080	310	0.97	11.97	230	0.0044
356	14	356.58	73.06	0.126	327	0.85	13.10	230	0.0042
356	16	356.67	72.36	0.143	349	0.92	12.18	214	0.0041
356	18	356.75	72.83	0.218	351	0.87	11.75	225	0.0040
356	20	356.83	73.10	0.182	356	0.90	11.83	222	0.0041
356	22	356.92	73.79	0.145	13	0.94	12.34	224	0.0032
357	0	357.00	73.55	0.077	94	0.78	11.73	237	0.0026
357	2	357.08	72.64	0.032	85	0.87	11.72	221	0.0028
357	4	357.17	72.33	0.081	328	0.76	11.51	222	0.0026
357	6	357.25	72.59	0.123	351	0.76	11.78	224	0.0025
357	8	357.33	73.24	0.119	1	0.63	11.39	221	0.0044
357	10	357.42	73.81	0.058	84	0.70	12.10	230	0.0023
357	12	357.50	73.71	0.080	122	0.70	11.86	233	0.0023
357	14	357.58	73.35	0.112	140	0.62	10.51	228	0.0022
357	16	357.67	72.43	0.031	132	0.51	11.11	236	0.0013
357	18	357.75	72.33	0.082	312	0.52	11.52	236	0.0015
357	20	357.83	73.13	0.084	353	0.51	11.11	222	0.0013
357	22	357.92	73.44	0.063	63	0.46	9.21	253	0.0014
358	0	358.00	73.49	0.133	112	0.46	8.64	270	0.0011
358	2	358.08	72.91	0.132	135	0.46	9.35	232	0.0010
358	4	358.17	72.38	0.060	183	0.46	11.32	218	0.0013
358	6	358.25	72.36	0.090	260	0.46	8.46	250	0.0008
358	8	358.33	72.88	0.142	295	0.50	9.72	246	0.0082
358	10	358.42	73.60	0.087	322	0.48	10.69	260	0.0007
358	12	358.50	74.19	0.036	143	0.41	11.32	220	0.0011
358	14	358.58	73.41	0.098	130	0.45	8.99	247	0.0011
358	16	358.67	72.86	0.048	173	0.45	10.46	232	0.0019
358	18	358.75	72.57	0.067	255	0.40	10.21	259	0.0035
358	20	358.83	72.88	0.057	265	0.45	10.40	255	0.0008
358	22	358.92	73.51	0.066	300	0.46	11.30	266	0.0009
359	0	359.00	73.86	0.054	96	0.47	9.42	304	0.0009
359	2	359.08	73.49	0.080	151	0.72	9.50	307	0.0011
359	4	359.17	72.69	0.051	213	1.35	10.03	332	0.0011
359	6	359.25	72.40	0.013	192	2.84	10.63	331	0.0045
359	8	359.33	72.70	0.071	345	2.12	11.12	333	0.0074
359	10	359.42	73.38	0.117	353	2.87	11.74	321	0.0128
359	12	359.50	73.65	0.111	59	3.56	11.24	331	0.0119
359	14	359.58	73.81	0.120	120	3.44	11.76	319	0.0146
359	16	359.67	73.12	0.107	134	4.39	11.48	325	0.0149
359	18	359.75	72.20	0.073	126	3.76	11.78	333	0.0200
359	20	359.83	72.56	0.007	201	3.33	11.41	333	0.0385
359	22	359.92	73.21	0.017	192	4.01	11.82	336	0.0332
360	0	360.00	73.50	0.070	160	2.39	11.36	334	0.0474
360	2	360.08	73.72	0.098	179	3.30	11.02	334	0.0220
360	4	360.17	73.14	0.110	179	2.55	10.75	338	0.0260
360	6	360.25	72.66	0.138	216	3.02	10.96	337	0.0266
360	8	360.33	72.45	0.184	225	2.90	10.41	339	0.0199
360	10	360.42	73.38	0.175	236	2.30	10.59	343	0.0286
360	12	360.50	74.03	0.184	223	2.37	10.66	338	0.0071
360	14	360.58	73.86	0.113	199	1.98	10.17	342	0.0094
360	16	360.67	73.58	0.126	205	1.86	10.06	340	0.0097
360	18	360.75	72.78	0.155	217	1.99	9.95	340	0.0106
360	20	360.83	72.28	0.172	261	2.28	8.24	356	0.0082
360	22	360.92	72.65	0.150	303	1.38	10.05	344	0.0084
361	0	361.00	73.27	0.095	322	1.27	9.84	353	0.0080
361	2	361.08	73.79	0.030	11	1.42	9.97	347	0.0084
361	4	361.17	73.02	0.026	86	0.91	10.15	350	0.0079
361	6	361.25	72.79	0.039	304	1.06	9.97	349	0.0073
361	8	361.33	72.40	0.011	209	0.58	9.96	341	0.0075
361	10	361.42	73.10	0.045	221	0.53	9.81	337	0.0075
361	12	361.50	73.46	0.110	199	0.57	8.29	342	0.0069
361	14	361.58	73.90	0.176	206	0.66	9.11	265	0.0062
361	16	361.67	73.88	0.242	206	0.46	8.34	330	0.0042
361	18	361.75	72.81	0.248	222	0.46	9.09	22	0.0045
361	20	361.83	72.39	0.269	244	0.44	8.90	337	0.0044

Day	Hour	YearDay	Depth	U100	Cdir	Hs	Tp	Wdir	OBS50
361	22	361.92	72.61	0.166	266	0.44	6.39	310	0.0030
362	0	362.00	73.42	0.159	277	0.46	8.79	332	0.0019
362	2	362.08	73.80	0.076	268	0.41	9.29	293	0.0017
362	4	362.17	73.36	0.033	213	0.42	10.32	246	0.0018
362	6	362.25	72.84	0.035	348	0.50	8.51	235	0.0014
362	8	362.33	72.45	0.037	265	0.88	9.45	232	0.0019
362	10	362.42	72.51	0.058	283	1.60	9.72	249	0.0021
362	12	362.50	73.03	0.091	272	1.17	9.72	251	0.0022
362	14	362.58	73.42	0.099	284	2.48	10.22	251	0.0023
362	16	362.67	73.29	0.102	316	1.43	9.85	292	0.0033
362	18	362.75	73.00	0.144	360	2.14	10.12	301	0.0076
362	20	362.83	72.06	0.256	11	1.89	9.50	308	0.0070
362	22	362.92	72.15	0.269	19	2.98	9.72	317	0.0059
363	0	363.00	73.02	0.221	46	2.23	9.34	331	0.0070
363	2	363.08	73.21	0.179	91	1.74	11.13	336	0.0119
363	4	363.17	73.73	0.192	125	1.67	9.80	345	0.0074
363	6	363.25	73.41	0.246	158	1.38	10.34	355	0.0072
363	8	363.33	72.95	0.298	201	1.91	10.24	356	0.0067
363	10	363.42	72.92	0.270	215	1.76	8.93	316	0.0084
363	12	363.50	72.99	0.233	235	1.52	10.62	341	0.0086
363	14	363.58	73.42	0.220	241	1.47	11.06	334	0.0059
363	16	363.67	73.93	0.188	229	1.43	10.98	336	0.0044
363	18	363.75	73.56	0.174	222	0.93	10.80	325	0.0036
363	20	363.83	72.69	0.111	239	1.30	11.06	331	0.0035
363	22	363.92	72.52	0.173	269	1.13	8.81	314	0.0039
364	0	364.00	73.12	0.180	268	1.06	7.17	283	0.0034
364	2	364.08	73.20	0.205	282	0.88	8.90	294	0.0026
364	4	364.17	73.50	0.102	267	0.77	9.87	282	0.0017
364	6	364.25	73.58	0.113	246	0.72	9.37	296	0.0017
364	8	364.33	72.82	0.119	242	0.67	9.67	251	0.0011
364	10	364.42	72.74	0.187	275	0.99	9.05	299	0.0013
364	12	364.50	72.61	0.196	300	0.77	9.94	299	0.0016
364	14	364.58	72.91	0.175	323	0.87	9.68	288	0.0020
364	16	364.67	73.37	0.209	347	0.95	9.05	321	0.0028
364	18	364.75	72.94	0.251	10	2.25	9.46	346	0.0040
364	20	364.83	72.48	0.254	11	2.93	10.22	333	0.0052
364	22	364.92	72.56	0.248	18	2.68	9.70	322	0.0046
365	0	365.00	72.78	0.127	49	2.11	9.49	329	0.0050
365	2	365.08	73.17	0.145	104	2.71	10.35	336	0.0043
365	4	365.17	73.32	0.131	141	2.81	10.34	340	0.0050
365	6	365.25	73.43	0.189	174	1.87	10.33	342	0.0053
365	8	365.33	73.38	0.226	195	2.20	9.50	349	0.0041
365	10	365.42	72.99	0.242	214	1.43	9.66	334	0.0036
365	12	365.50	72.98	0.185	241	1.96	10.12	345	0.0040
365	14	365.58	73.22	0.127	267	1.73	9.49	339	0.0032
365	16	365.67	73.57	0.109	284	1.62	10.82	335	0.0026
365	18	365.75	73.63	0.024	294	1.30	11.06	339	0.0021
365	20	365.83	73.01	0.040	15	1.08	11.10	338	0.0024
365	22	365.92	72.97	0.045	324	0.84	10.73	303	0.0021
366	0	366.00	72.99	0.057	306	1.04	9.61	290	0.0023
366	2	366.08	73.16	0.038	255	1.39	9.68	281	0.0025
366	4	366.17	73.46	0.060	257	1.54	9.90	280	0.0024
366	6	366.25	73.57	0.083	263	1.89	9.69	355	0.0027
366	8	366.33	72.80	0.143	4	7.63	11.32	6	0.0128
366	10	366.42	72.23	0.457	37	8.50	11.19	14	0.0487
366	12	366.50	72.17	0.394	57	6.30	11.70	20	0.1021
366	14	366.58	72.77	0.429	77	6.22	11.54	36	0.0245
366	16	366.67	72.79	0.432	110	5.41	11.02	19	0.0096
366	18	366.75	73.48	0.410	141	4.33	11.45	15	0.0074
366	20	366.83	73.47	0.380	153	3.04	10.81	3	0.0055
366	22	366.92	73.27	0.512	183	2.99	10.23	0	0.0181
367	0	367.00	73.13	0.471	198	2.98	9.02	348	0.0270
367	2	367.08	73.15	0.467	235	2.42	10.51	355	0.0137
367	4	367.17	73.52	0.303	258	2.24	10.03	344	0.0113
367	6	367.25	73.36	0.179	276	2.30	10.48	348	0.0098
367	8	367.33	73.34	0.104	325	2.13	11.06	349	0.0098
367	10	367.42	73.08	0.195	20	1.36	10.33	339	0.0077
367	12	367.50	72.80	0.121	51	1.69	10.67	341	0.0120
367	14	367.58	73.13	0.078	94	1.43	10.68	330	0.0112
367	16	367.67	73.34	0.026	236	1.45	9.89	297	0.0114
367	18	367.75	73.31	0.165	219	1.60	10.06	298	0.0111
367	20	367.83	73.55	0.168	243	1.22	10.23	283	0.0081
367	22	367.92	73.25	0.128	276	1.55	9.88	288	0.0054
368	0	368.00	72.54	0.177	332	1.18	11.01	294	0.0069
368	2	368.08	72.53	0.336	1	1.94	8.51	323	0.0132
368	4	368.17	72.67	0.293	8	2.71	9.50	359	0.0129
368	6	368.25	72.98	0.232	21	4.99	11.27	26	0.0219
368	8	368.33	73.17	0.215	62	4.14	10.97	18	0.0169
368	10	368.42	73.05	0.361	103	3.56	10.93	25	0.0082
368	12	368.50	72.81	0.321	122	4.06	10.79	21	0.0068
368	14	368.58	72.73	0.297	168	3.36	10.81	353	0.0082

Day	Hour	YearDay	Depth	U100	Cdir	Hs	Tp	Wdir	OBS50
368	16	368.67	73.14	0.249	189	2.97	10.10	337	0.0100
368	18	368.75	73.10	0.221	218	2.68	9.85	329	0.0124
368	20	368.83	73.58	0.171	228	2.42	10.73	324	0.0110
368	22	368.92	73.25	0.109	245	2.89	10.30	325	0.0099
369	0	369.00	73.19	0.082	208	2.58	10.29	319	0.0090
369	2	369.08	72.95	0.072	245	1.96	10.14	313	0.0090
369	4	369.17	72.76	0.078	260	1.48	10.23	320	0.0093
369	6	369.25	73.19	0.077	258	1.55	10.11	326	0.0089
369	8	369.33	73.80	0.088	234	1.25	10.75	319	0.0085
369	10	369.42	73.44	0.099	222	1.18	10.70	323	0.0072
369	12	369.50	73.00	0.116	219	1.34	11.18	310	0.0068
369	14	369.58	73.03	0.161	237	1.01	10.96	305	0.0084
369	16	369.67	72.65	0.081	251	1.08	10.28	293	0.0072
369	18	369.75	72.79	0.070	294	0.82	10.97	307	0.0064
369	20	369.83	73.12	0.071	337	0.88	11.68	289	0.0061
369	22	369.92	73.48	0.056	6	0.84	11.15	317	0.0061
370	0	370.00	73.17	0.052	52	0.76	11.31	292	0.0071
370	2	370.08	72.85	0.083	18	0.63	11.07	289	0.0051
370	4	370.17	72.60	0.093	8	0.68	11.64	289	0.0045
370	6	370.25	72.90	0.097	356	0.63	10.80	290	0.0047
370	8	370.33	73.60	0.073	38	0.56	9.90	333	0.0041
370	10	370.42	73.43	0.122	88	0.63	9.17	33	0.0038
370	12	370.50	73.15	0.146	89	1.00	9.52	32	0.0077
370	14	370.58	72.73	0.145	102	1.11	9.47	38	0.0048
370	16	370.67	72.50	0.108	111	0.90	10.25	30	0.0042
370	18	370.75	72.66	0.064	124	0.72	9.98	12	0.0047
370	20	370.83	73.37	0.031	136	0.65	9.63	18	0.0038
370	22	370.92	73.32	0.105	140	0.81	9.48	19	0.0044
371	0	371.00	73.15	0.152	159	0.73	8.21	17	0.0055
371	2	371.08	72.79	0.208	189	0.70	8.59	26	0.0080
371	4	371.17	72.66	0.246	212	0.68	9.09	338	0.0104
371	6	371.25	72.89	0.257	242	0.53	9.34	12	0.0066
371	8	371.33	73.65	0.264	251	0.52	8.85	260	0.0056
371	10	371.42	73.96	0.163	227	0.51	10.61	292	0.0053
371	12	371.50	73.48	0.107	220	0.46	11.86	292	0.0042
371	14	371.58	73.02	0.107	230	0.54	11.06	267	0.0042
371	16	371.67	72.62	0.129	258	0.62	8.54	308	0.0041
371	18	371.75	72.61	0.147	268	0.42	6.65	299	0.0030
371	20	371.83	73.03	0.142	277	0.51	10.10	297	0.0031
371	22	371.92	73.40	0.069	264	0.57	11.45	283	0.0034
372	0	372.00	73.58	0.038	219	0.47	11.30	283	0.0028
372	2	372.08	72.81	0.053	231	0.58	11.07	285	0.0029
372	4	372.17	72.52	0.080	275	0.46	13.65	252	0.0034
372	6	372.25	72.67	0.110	329	0.52	11.10	261	0.0026
372	8	372.33	73.41	0.141	329	0.51	10.31	274	0.0024
372	10	372.42	73.89	0.114	350	0.48	10.25	302	0.0030
372	12	372.50	73.90	0.104	27	0.42	12.32	254	0.0025
372	14	372.58	73.48	0.076	93	0.42	12.00	259	0.0025
372	16	372.67	72.91	0.002	198	0.40	13.71	254	0.0025
372	18	372.75	72.79	0.091	325	0.48	12.08	244	0.0025
372	20	372.83	72.83	0.113	346	0.40	9.25	283	0.0102
372	22	372.92	73.33	0.095	358	0.53	10.33	265	0.0021
373	0	373.00	73.40	0.088	61	0.57	8.59	290	0.0019
373	2	373.08	72.96	0.102	95	0.52	10.89	298	0.0016
373	4	373.17	72.53	0.044	39	0.51	11.89	280	0.0016
373	6	373.25	72.81	0.089	339	0.51	10.74	282	0.0013
373	8	373.33	73.22	0.129	353	0.52	11.44	274	0.0012
373	10	373.42	73.44	0.113	10	0.59	10.12	271	0.0011
373	12	373.50	73.96	0.087	59	0.52	9.83	302	0.0016
373	14	373.58	73.35	0.132	103	0.51	9.47	264	0.0016
373	16	373.67	72.99	0.086	138	0.57	10.42	283	0.0017
373	18	373.75	72.42	0.021	291	0.42	11.90	289	0.0015
373	20	373.83	73.02	0.079	342	0.49	11.86	271	0.0016
373	22	373.92	73.50	0.046	6	0.47	13.19	255	0.0024
374	0	374.00	73.54	0.082	97	0.43	12.45	243	0.0029
374	2	374.08	73.48	0.092	130	0.44	10.21	252	0.0014
374	4	374.17	73.01	0.065	176	0.42	10.69	280	0.0015
374	6	374.25	72.80	0.082	278	0.54	11.06	271	0.0014
374	8	374.33	73.09	0.100	295	0.51	11.55	252	0.0014
374	10	374.42	73.39	0.078	330	0.42	10.40	249	0.0010
374	12	374.50	73.77	0.033	18	0.43	11.66	255	0.0011
374	14	374.58	73.88	0.081	140	0.50	10.57	267	0.0011
374	16	374.67	73.23	0.098	180	0.43	9.47	261	0.0013
374	18	374.75	72.73	0.070	279	0.43	10.90	272	0.0014
374	20	374.83	72.47	0.111	328	0.51	9.91	279	0.0012
374	22	374.92	73.37	0.144	351	0.40	9.54	244	0.0012
375	0	375.00	73.41	0.135	26	0.51	10.47	265	0.0008
375	2	375.08	73.30	0.141	82	0.40	9.35	279	0.0008
375	4	375.17	73.02	0.126	111	0.44	8.78	259	0.0008
375	6	375.25	72.35	0.071	104	0.43	11.45	249	0.0009
375	8	375.33	72.52	0.074	26	0.44	10.73	263	0.0009

Day	Hour	YearDay	Depth	U100	Cdir	Hs	Tp	Wdir	OBS50
375	10	375.42	73.05	0.088	8	0.46	9.79	282	0.0006
375	12	375.50	73.89	0.095	24	0.38	10.13	290	0.0011
375	14	375.58	73.61	0.139	79	0.49	9.60	307	0.0003
375	16	375.67	72.96	0.176	105	0.36	7.60	348	0.0004
375	18	375.75	72.36	0.081	81	0.48	9.82	272	0.0002
375	20	375.83	72.31	0.117	19	0.49	9.39	299	0.0013
375	22	375.92	73.07	0.146	19	0.53	9.05	21	0.0002
376	0	376.00	73.33	0.130	64	0.42	7.73	7	0.0001
376	2	376.08	73.41	0.176	94	0.56	8.32	4	0.0001
376	4	376.17	73.28	0.165	130	0.65	7.58	350	0.0002
376	6	376.25	72.48	0.173	147	0.93	9.42	2	0.0004
376	8	376.33	72.72	0.072	161	0.97	9.87	348	0.0008
376	10	376.42	72.90	0.036	214	1.27	10.29	351	0.0026
376	12	376.50	73.82	0.055	203	1.42	10.30	350	0.0014
376	14	376.58	73.75	0.029	143	1.62	9.94	48	0.0026
376	16	376.67	73.31	0.139	174	1.58	9.82	30	0.0037
376	18	376.75	72.95	0.109	195	1.68	9.71	48	0.0023
376	20	376.83	72.46	0.121	237	1.60	10.45	60	0.0014
376	22	376.92	73.15	0.169	249	1.07	10.59	54	0.0013
377	0	377.00	73.68	0.156	223	1.36	10.10	30	0.0013
377	2	377.08	73.69	0.185	203	0.66	7.85	8	0.0019
377	4	377.17	73.37	0.164	201	0.52	7.89	5	0.0018
377	6	377.25	72.75	0.171	214	0.69	8.62	350	0.0012
377	8	377.33	72.81	0.213	265	0.58	7.10	300	0.0016
377	10	377.42	73.09	0.230	283	0.46	8.08	30	0.0007
377	12	377.50	73.35	0.221	319	0.45	8.94	6	0.0007
377	14	377.58	73.73	0.145	343	0.53	9.35	323	0.0002
377	16	377.67	73.44	0.052	62	0.44	8.02	338	0.0006
377	18	377.75	72.69	0.077	42	0.42	9.37	304	0.0005
377	20	377.83	72.27	0.149	353	0.49	9.30	311	0.0006
377	22	377.92	72.79	0.218	355	0.39	7.57	290	0.0009
378	0	378.00	72.96	0.207	12	0.37	9.12	263	0.0018
378	2	378.08	73.38	0.221	30	0.46	9.34	259	0.0013
378	4	378.17	73.28	0.180	54	0.48	8.47	319	0.0009
378	6	378.25	72.74	0.164	60	0.43	7.18	259	0.0008
378	8	378.33	72.33	0.169	42	0.40	9.43	242	0.0006
378	10	378.42	72.77	0.153	40	0.61	10.27	249	0.0001
378	12	378.50	73.03	0.112	59	0.45	8.18	241	0.0003
378	14	378.58	73.59	0.140	95	0.48	10.86	196	0.0004
378	16	378.67	73.61	0.216	140	0.64	10.12	199	0.0002
378	18	378.75	73.02	0.275	152	0.49	9.88	216	0.0006
378	20	378.83	72.53	0.148	179	0.55	8.95	187	0.0007
378	22	378.92	72.58	0.095	222	0.52	10.83	285	0.0006
379	0	379.00	73.32	0.053	261	0.62	9.24	354	0.0006
379	2	379.08	73.75	0.006	215	0.48	10.81	354	0.0003
379	4	379.17	73.60	0.041	166	0.56	9.48	51	0.0005
379	6	379.25	73.53	0.072	140	0.63	9.34	58	0.0003
379	8	379.33	72.91	0.037	48	0.69	9.43	55	0.0003
379	10	379.42	72.87	0.029	152	0.70	10.13	46	0.0009
379	12	379.50	72.91	0.141	256	0.82	8.60	72	0.0005
379	14	379.58	73.77	0.131	249	0.58	9.96	65	0.0004
379	16	379.67	73.67	0.084	230	0.52	9.80	64	0.0006
379	18	379.75	73.19	0.156	213	0.70	9.42	63	0.0005
379	20	379.83	72.64	0.175	233	0.52	10.19	44	0.0005
379	22	379.92	72.53	0.154	271	0.47	6.02	359	0.0003
380	0	380.00	72.83	0.175	311	0.41	8.59	18	0.0004
380	2	380.08	73.59	0.135	332	0.37	9.93	321	0.0002
380	4	380.17	73.54	0.078	357	0.34	10.23	312	0.0003
380	6	380.25	73.36	0.027	51	0.40	9.89	258	0.0001
380	8	380.33	73.15	0.014	198	0.50	9.71	237	0.0002
380	10	380.42	72.80	0.067	313	0.48	8.75	273	0.0002
380	12	380.50	72.92	0.118	360	1.22	9.34	280	0.0001
380	14	380.58	73.09	0.080	349	1.03	9.52	279	0.0001
380	16	380.67	73.66	0.058	73	0.70	9.30	275	0.0001
380	18	380.75	73.47	0.071	88	1.20	9.88	271	0.0002
380	20	380.83	72.63	0.118	63	0.70	9.41	266	0.0000
380	22	380.92	72.66	0.164	79	0.70	10.16	265	0.0000
381	0	381.00	72.82	0.099	75	2.12	9.77	349	0.0001
381	2	381.08	72.93	0.039	47	4.78	11.14	3	0.0215
381	4	381.17	73.32	0.035	11	4.17	12.53	7	0.0505
381	6	381.25	73.66	0.106	99	3.76	12.10	359	0.0489
381	8	381.33	72.95	0.116	127	4.27	11.91	7	0.0266
381	10	381.42	72.50	0.050	148	3.91	11.90	4	0.0311
381	12	381.50	72.41	0.022	113	2.56	11.73	4	0.0325
381	14	381.58	73.10	0.031	150	2.69	11.52	5	0.0433
381	16	381.67	73.18	0.058	142	2.54	11.28	5	0.0430
381	18	381.75	73.61	0.113	136	2.22	10.86	0	0.0344
381	20	381.83	72.97	0.161	150	2.16	10.63	4	0.0198
381	22	381.92	72.59	0.100	192	1.33	10.56	359	0.0130

Appendix 2: Bottom boundary layer dynamics parameters predicted by SEDTRANS96 for 2007 Green Bank deployment: burst number (bt#), near-bed wave orbital velocity (u_b , cm/s), near-bed wave orbital amplitude (A_b , cm), combined wave-current friction factor (fcws), thickness of the wave-current boundary layer (D_{cw} , cm), skin friction current shear velocity (u^*_{cs} , cm/s), skin friction wave shear velocity (u^*_{ws} , cm/s), skin friction combined wave-current shear velocity (u^*_{cws} , cm/s), total current shear velocity (u^*_c , cm/s), total wave shear velocity (u^*_w , cm/s), total combined wave-current shear velocity (u^*_{cw} , cm/s), bottom roughness (z_0 , cm), and apparent bottom roughness (z_{0c} , cm).

Appendix 3: Ripple metrics and sediment transport parameters predicted by SEDTRANS96 for 2007 Green Bank deployment: burst number (bt#), predicted ripple height (H_r , cm), predicted ripple wavelength (L_r , cm), Einstein-Brown bedload transport rate (Q_b , $\text{kg m}^{-1} \text{s}^{-1}$), bedload transport direction (Q_{bdir}), suspended sediment concentration averaged over the bottom 2 m (C_{avg} , g l^{-1}), suspended load sediment transport rate (Q_s , $\text{kg m}^{-1} \text{s}^{-1}$), and suspended load transport direction (taken as the mean current direction, C_{dir}).

BT#	YearDay	Hr	Lr	Qb	Qbdir	Cavg	Qs	Cdir
1	341.67	0	0	0	0	0	0	211
2	341.75	0	0	0	0	0	0	259
3	341.83	0	0	0	0	0	0	260
4	341.92	0	0	0	0	0	0	273
5	342.00	0	0	0	0	0	0	259
6	342.08	0	0	0	0	0	0	260
7	342.17	0	0	0	0	0	0	266
8	342.25	0	0	0	0	0	0	326
9	342.33	0	0	0	0	0	0	320
10	342.42	0	0	0	0	0	0	246
11	342.50	0	0	0	0	0	0	230
12	342.58	0	0	0	0	0	0	222
13	342.67	0	0	0	0	0	0	280
14	342.75	0	0	0	0	0	0	335
15	342.83	0	0	0	0	0	0	17
16	342.92	0	0	0	0	0	0	72
17	343.00	0	0	0	0	0	0	74
18	343.08	0	0	0	0	0	0	64
19	343.17	0	0	0	0	0	0	43
20	343.25	0	0	0	0	0	0	39
21	343.33	0	0	0	0	0	0	45
22	343.42	0	0	0	0	0	0	76
23	343.50	0	0	0	0	0	0	107
24	343.58	0	0	0	0	0	0	151
25	343.67	0	0	0	0	0	0	184
26	343.75	0	0	0	0	0	0	206
27	343.83	0	0	0	0	0	0	247
28	343.92	0	0	0	0	0	0	248
29	344.00	0	0	0	0	0	0	209
30	344.08	0	0	0	0	0	0	140
31	344.17	0	0	0	0	0	0	151
32	344.25	0	0	0	0	0	0	214
33	344.33	0	0	0	0	0	0	270
34	344.42	0	0	0	0	0	0	220
35	344.50	0	0	0	0	0	0	220
36	344.58	0	0	0	0	0	0	215
37	344.67	0	0	0	0	0	0	228
38	344.75	0	0	0	0	0	0	265
39	344.83	0	0	0	0	0	0	286
40	344.92	0	0	0	0	0	0	335
41	345.00	0	0	0	0	0	0	357
42	345.08	0	0	0	0	0	0	50
43	345.17	0	0	0	0	0	0	134
44	345.25	0	0	0	0	0	0	274
45	345.33	0	0	0	0	0	0	323
46	345.42	0	0	0	0	0	0	307
47	345.50	0	0	0	0	0	0	3
48	345.58	0	0	0	0	0	0	90
49	345.67	0	0	0	0	0	0	189
50	345.75	0	0	0	0	0	0	266
51	345.83	0	0	0	0	0	0	296
52	345.92	0	0	0	0	0	0	289
53	346.00	0	0	0	0	0	0	334
54	346.08	0	0	0	0	0	0	175
55	346.17	0	0	0	0	0	0	194
56	346.25	0	0	0	0	0	0	248
57	346.33	0	0	0	0	0	0	269
58	346.42	0	0	0	0	0	0	290
59	346.50	0	0	0	0	0	0	308
60	346.58	0	0	0	0	0	0	246
61	346.67	0	0	0	0	0	0	191
62	346.75	0	0	0	0	0	0	238
63	346.83	0	0	0	0	0	0	271
64	346.92	0	0	0	0	0	0	300
65	347.00	0	0	0	0	0	0	335
66	347.08	0	0	0	0	0	0	354
67	347.17	0	0	0	0	0	0	7
68	347.25	0	0	0	0	0	0	353
69	347.33	1.54	15.9	0.000508	47	0	0	357
70	347.42	0	0	0.002309	45	0.011249	0.000141	7
71	347.50	1.45	15.9	0.000356	46	0	0	24
72	347.58	1.7	11.33	0.000033	96	0	0	77
73	347.67	1.54	10.27	0.000028	183	0	0	126
74	347.75	1.7	11.32	0.000094	205	0	0	163
75	347.83	1.55	10.31	0.000035	222	0	0	203
76	347.92	1.29	10.74	0.000118	270	0	0	232
77	348.00	0	0	0	0	0	0	241
78	348.08	0	0	0	0	0	0	274
79	348.17	0	0	0	0	0	0	258
80	348.25	0	0	0	0	0	0	311
81	348.33	0	0	0	0	0	0	290

BT#	YearDay	Hr	Lr	Qb	Qbdir	Cavg	Qs	Cdir
82	348.42	0	0	0	0	0	0	279
83	348.50	0	0	0	0	0	0	258
84	348.58	0	0	0	0	0	0	237
85	348.67	0	0	0	0	0	0	233
86	348.75	0	0	0	0	0	0	259
87	348.83	0	0	0	0	0	0	281
88	348.92	0	0	0	0	0	0	308
89	349.00	0	0	0	0	0	0	330
90	349.08	0	0	0	0	0	0	333
91	349.17	0	0	0	0	0	0	354
92	349.25	0	0	0	0	0	0	12
93	349.33	0	0	0	0	0	0	323
94	349.42	0	0	0	0	0	0	331
95	349.50	0	0	0	0	0	0	300
96	349.58	0	0	0	0	0	0	286
97	349.67	0	0	0	0	0	0	278
98	349.75	0	0	0	0	0	0	298
99	349.83	0	0	0	0	0	0	334
100	349.92	0	0	0	0	0	0	336
101	350.00	0	0	0	0	0	0	13
102	350.08	0	0	0	0	0	0	19
103	350.17	0	0	0	0	0	0	40
104	350.25	0	0	0	0	0	0	131
105	350.33	0	0	0	0	0	0	189
106	350.42	0	0	0	0	0	0	265
107	350.50	0	0	0	0	0	0	291
108	350.58	0	0	0	0	0	0	318
109	350.67	0	0	0	0	0	0	357
110	350.75	0	0	0	0	0	0	160
111	350.83	0	0	0	0	0	0	251
112	350.92	0	0	0	0	0	0	253
113	351.00	0	0	0	0	0	0	272
114	351.08	0	0	0	0	0	0	311
115	351.17	0	0	0	0	0	0	281
116	351.25	0	0	0	0	0	0	294
117	351.33	0	0	0	0	0	0	346
118	351.42	0	0	0	0	0	0	341
119	351.50	0	0	0	0	0	0	340
120	351.58	1.55	10.34	0.000005	260	0	0	218
121	351.67	1.6	10.66	0.000045	279	0	0	238
122	351.75	1.98	15.9	0.000117	328	0	0	312
123	351.83	2.14	15.9	0.000121	28	0	0	355
124	351.92	0.53	15.9	0.001028	61	0	0	5
125	352.00	1.13	15.9	0.000672	83	0	0	19
126	352.08	0.48	15.9	0.000692	96	0	0	23
127	352.17	1.31	15.9	0.000236	71	0	0	22
128	352.25	0	0	0.001	137	0.060102	0.000134	53
129	352.33	0	0	0.001098	147	0.038815	0.000104	74
130	352.42	0	0	0.000429	145	0.01223	0.000024	75
131	352.50	0.39	15.9	0.000244	19	0	0	358
132	352.58	0	0	0.000343	75	0.036261	0.000057	33
133	352.67	0.46	15.9	0.000123	105	0	0	42
134	352.75	0.35	15.9	0.000305	152	0	0	71
135	352.83	0.85	15.9	0.000287	171	0	0	112
136	352.92	1.81	15.9	0.000168	174	0	0	118
137	353.00	1.6	10.66	0.000011	197	0	0	172
138	353.08	0	0	0	0	0	0	205
139	353.17	0	0	0	0	0	0	212
140	353.25	0	0	0	0	0	0	212
141	353.33	0	0	0	0	0	0	200
142	353.42	0	0	0	0	0	0	205
143	353.50	0	0	0	0	0	0	225
144	353.58	0	0	0	0	0	0	258
145	353.67	0	0	0	0	0	0	265
146	353.75	0	0	0	0	0	0	309
147	353.83	0	0	0	0	0	0	248
148	353.92	0	0	0	0	0	0	173
149	354.00	0	0	0	0	0	0	236
150	354.08	0	0	0	0	0	0	274
151	354.17	0	0	0	0	0	0	308
152	354.25	0	0	0	0	0	0	305
153	354.33	0	0	0	0	0	0	328
154	354.42	0	0	0	0	0	0	354
155	354.50	0	0	0	0	0	0	341
156	354.58	0	0	0	0	0	0	335
157	354.67	0	0	0	0	0	0	199
158	354.75	0	0	0	0	0	0	247
159	354.83	0	0	0	0	0	0	257
160	354.92	0	0	0	0	0	0	256
161	355.00	0	0	0	0	0	0	281
162	355.08	0	0	0	0	0	0	324

BT#	YearDay	Hr	Lr	Qb	Qbdir	Cavg	Qs	Cdir
163	355.17	0	0	0	0	0	0	326
164	355.25	0	0	0	0	0	0	329
165	355.33	0	0	0	0	0	0	293
166	355.42	0	0	0	0	0	0	35
167	355.50	0	0	0	0	0	0	224
168	355.58	0	0	0	0	0	0	268
169	355.67	0	0	0	0	0	0	303
170	355.75	0	0	0	0	0	0	316
171	355.83	0	0	0	0	0	0	312
172	355.92	0	0	0	0	0	0	263
173	356.00	0	0	0	0	0	0	305
174	356.08	0	0	0	0	0	0	301
175	356.17	0	0	0	0	0	0	287
176	356.25	0	0	0	0	0	0	290
177	356.33	0	0	0	0	0	0	320
178	356.42	0	0	0	0	0	0	301
179	356.50	0	0	0	0	0	0	310
180	356.58	0	0	0	0	0	0	327
181	356.67	0	0	0	0	0	0	349
182	356.75	0	0	0	0	0	0	351
183	356.83	0	0	0	0	0	0	356
184	356.92	0	0	0	0	0	0	13
185	357.00	0	0	0	0	0	0	94
186	357.08	0	0	0	0	0	0	85
187	357.17	0	0	0	0	0	0	328
188	357.25	0	0	0	0	0	0	351
189	357.33	0	0	0	0	0	0	1
190	357.42	0	0	0	0	0	0	84
191	357.50	0	0	0	0	0	0	122
192	357.58	0	0	0	0	0	0	140
193	357.67	0	0	0	0	0	0	132
194	357.75	0	0	0	0	0	0	312
195	357.83	0	0	0	0	0	0	353
196	357.92	0	0	0	0	0	0	63
197	358.00	0	0	0	0	0	0	112
198	358.08	0	0	0	0	0	0	135
199	358.17	0	0	0	0	0	0	183
200	358.25	0	0	0	0	0	0	260
201	358.33	0	0	0	0	0	0	295
202	358.42	0	0	0	0	0	0	322
203	358.50	0	0	0	0	0	0	143
204	358.58	0	0	0	0	0	0	130
205	358.67	0	0	0	0	0	0	173
206	358.75	0	0	0	0	0	0	255
207	358.83	0	0	0	0	0	0	265
208	358.92	0	0	0	0	0	0	300
209	359.00	0	0	0	0	0	0	96
210	359.08	0	0	0	0	0	0	151
211	359.17	0	0	0	0	0	0	213
212	359.25	0	0	0	0	0	0	192
213	359.33	0	0	0	0	0	0	345
214	359.42	1.52	10.12	0.000015	28	0	0	353
215	359.50	1.67	11.12	0.000044	134	0	0	59
216	359.58	2.2	15.9	0.0001	146	0	0	120
217	359.67	1.46	15.9	0.000186	155	0	0	134
218	359.75	2.06	15.9	0.000062	156	0	0	126
219	359.83	1.6	10.65	0.000001	168	0	0	201
220	359.92	2.1	15.9	0.000005	184	0	0	192
221	360.00	0	0	0	0	0	0	160
222	360.08	1.58	10.53	0.000018	192	0	0	179
223	360.17	0	0	0	0	0	0	179
224	360.25	1.52	10.15	0.000022	296	0	0	216
225	360.33	1.47	9.8	0.000026	299	0	0	225
226	360.42	0	0	0	0	0	0	236
227	360.50	0	0	0	0	0	0	223
228	360.58	0	0	0	0	0	0	199
229	360.67	0	0	0	0	0	0	205
230	360.75	0	0	0	0	0	0	217
231	360.83	0	0	0	0	0	0	261
232	360.92	0	0	0	0	0	0	303
233	361.00	0	0	0	0	0	0	322
234	361.08	0	0	0	0	0	0	11
235	361.17	0	0	0	0	0	0	86
236	361.25	0	0	0	0	0	0	304
237	361.33	0	0	0	0	0	0	209
238	361.42	0	0	0	0	0	0	221
239	361.50	0	0	0	0	0	0	199
240	361.58	0	0	0	0	0	0	206
241	361.67	0	0	0	0	0	0	206
242	361.75	0	0	0	0	0	0	222
243	361.83	4.24	30	0.00012	294	0	0	244

BT#	YearDay	Hr	Lr	Qb	Qbdir	Cavg	Qs	Cdir
244	361.92	0	0	0	0	0	0	266
245	362.00	0	0	0	0	0	0	277
246	362.08	0	0	0	0	0	0	268
247	362.17	0	0	0	0	0	0	213
248	362.25	0	0	0	0	0	0	348
249	362.33	0	0	0	0	0	0	265
250	362.42	0	0	0	0	0	0	283
251	362.50	0	0	0	0	0	0	272
252	362.58	0	0	0	0	0	0	284
253	362.67	0	0	0	0	0	0	316
254	362.75	0	0	0	0	0	0	360
255	362.83	0	0	0	0	0	0	11
256	362.92	0.99	8.22	0.000048	80	0	0	19
257	363.00	0	0	0	0	0	0	46
258	363.08	0	0	0	0	0	0	91
259	363.17	0	0	0	0	0	0	125
260	363.25	0	0	0	0	0	0	158
261	363.33	0	0	0	0	0	0	201
262	363.42	0	0	0	0	0	0	215
263	363.50	0	0	0	0	0	0	235
264	363.58	0	0	0	0	0	0	241
265	363.67	0	0	0	0	0	0	229
266	363.75	0	0	0	0	0	0	222
267	363.83	0	0	0	0	0	0	239
268	363.92	0	0	0	0	0	0	269
269	364.00	0	0	0	0	0	0	268
270	364.08	0	0	0	0	0	0	282
271	364.17	0	0	0	0	0	0	267
272	364.25	0	0	0	0	0	0	246
273	364.33	0	0	0	0	0	0	242
274	364.42	0	0	0	0	0	0	275
275	364.50	0	0	0	0	0	0	300
276	364.58	0	0	0	0	0	0	323
277	364.67	0	0	0	0	0	0	347
278	364.75	0	0	0	0	0	0	10
279	364.83	0	0	0	0	0	0	11
280	364.92	0	0	0	0	0	0	18
281	365.00	0	0	0	0	0	0	49
282	365.08	0	0	0	0	0	0	104
283	365.17	0	0	0	0	0	0	141
284	365.25	0	0	0	0	0	0	174
285	365.33	0	0	0	0	0	0	195
286	365.42	0	0	0	0	0	0	214
287	365.50	0	0	0	0	0	0	241
288	365.58	0	0	0	0	0	0	267
289	365.67	0	0	0	0	0	0	284
290	365.75	0	0	0	0	0	0	294
291	365.83	0	0	0	0	0	0	15
292	365.92	0	0	0	0	0	0	324
293	366.00	0	0	0	0	0	0	306
294	366.08	0	0	0	0	0	0	255
295	366.17	0	0	0	0	0	0	257
296	366.25	0	0	0	0	0	0	263
297	366.33	0	0	0.00084	31	0.014045	0.000054	4
298	366.42	0	0	0.005738	70	0.045408	0.001782	37
299	366.50	0.08	15.9	0.001665	89	0	0	57
300	366.58	0.5	15.9	0.001556	122	0	0	77
301	366.67	0	0	0.00353	175	0.017648	0.000495	110
302	366.75	0.36	15.9	0.002023	191	0	0	141
303	366.83	1.97	15.9	0.000437	195	0	0	153
304	366.92	1.69	15.9	0.001091	224	0	0	183
305	367.00	1.44	12.02	0.000462	252	0	0	198
306	367.08	2.22	15.9	0.000592	289	0	0	235
307	367.17	0.95	7.94	0.000055	311	0	0	258
308	367.25	0	0	0	0	0	0	276
309	367.33	0	0	0	0	0	0	325
310	367.42	0	0	0	0	0	0	20
311	367.50	0	0	0	0	0	0	51
312	367.58	0	0	0	0	0	0	94
313	367.67	0	0	0	0	0	0	236
314	367.75	0	0	0	0	0	0	219
315	367.83	0	0	0	0	0	0	243
316	367.92	0	0	0	0	0	0	276
317	368.00	0	0	0	0	0	0	332
318	368.08	0	0	0	0	0	0	1
319	368.17	0	0	0	0	0	0	8
320	368.25	1.57	15.9	0.000334	45	0	0	21
321	368.33	1.59	10.61	0.00005	110	0	0	62
322	368.42	2.06	15.9	0.000344	160	0	0	103
323	368.50	1.82	15.9	0.000387	182	0	0	122
324	368.58	1.92	15.9	0.000318	197	0	0	168

BT#	YearDay	Hr	Lr	Qb	Qbdir	Cavg	Qs	Cdir
325	368.67	0	0	0	0	0	0	189
326	368.75	0	0	0	0	0	0	218
327	368.83	0	0	0	0	0	0	228
328	368.92	0	0	0	0	0	0	245
329	369.00	0	0	0	0	0	0	208
330	369.08	0	0	0	0	0	0	245
331	369.17	0	0	0	0	0	0	260
332	369.25	0	0	0	0	0	0	258
333	369.33	0	0	0	0	0	0	234
334	369.42	0	0	0	0	0	0	222
335	369.50	0	0	0	0	0	0	219
336	369.58	0	0	0	0	0	0	237
337	369.67	0	0	0	0	0	0	251
338	369.75	0	0	0	0	0	0	294
339	369.83	0	0	0	0	0	0	337
340	369.92	0	0	0	0	0	0	6
341	370.00	0	0	0	0	0	0	52
342	370.08	0	0	0	0	0	0	18
343	370.17	0	0	0	0	0	0	8
344	370.25	0	0	0	0	0	0	356
345	370.33	0	0	0	0	0	0	38
346	370.42	0	0	0	0	0	0	88
347	370.50	0	0	0	0	0	0	89
348	370.58	0	0	0	0	0	0	102
349	370.67	0	0	0	0	0	0	111
350	370.75	0	0	0	0	0	0	124
351	370.83	0	0	0	0	0	0	136
352	370.92	0	0	0	0	0	0	140
353	371.00	0	0	0	0	0	0	159
354	371.08	0	0	0	0	0	0	189
355	371.17	0	0	0	0	0	0	212
356	371.25	0	0	0	0	0	0	242
357	371.33	0	0	0	0	0	0	251
358	371.42	0	0	0	0	0	0	227
359	371.50	0	0	0	0	0	0	220
360	371.58	0	0	0	0	0	0	230
361	371.67	0	0	0	0	0	0	258
362	371.75	0	0	0	0	0	0	268
363	371.83	0	0	0	0	0	0	277
364	371.92	0	0	0	0	0	0	264
365	372.00	0	0	0	0	0	0	219
366	372.08	0	0	0	0	0	0	231
367	372.17	0	0	0	0	0	0	275
368	372.25	0	0	0	0	0	0	329
369	372.33	0	0	0	0	0	0	329
370	372.42	0	0	0	0	0	0	350
371	372.50	0	0	0	0	0	0	27
372	372.58	0	0	0	0	0	0	93
373	372.67	0	0	0	0	0	0	198
374	372.75	0	0	0	0	0	0	325
375	372.83	0	0	0	0	0	0	346
376	372.92	0	0	0	0	0	0	358
377	373.00	0	0	0	0	0	0	61
378	373.08	0	0	0	0	0	0	95
379	373.17	0	0	0	0	0	0	39
380	373.25	0	0	0	0	0	0	339
381	373.33	0	0	0	0	0	0	353
382	373.42	0	0	0	0	0	0	10
383	373.50	0	0	0	0	0	0	59
384	373.58	0	0	0	0	0	0	103
385	373.67	0	0	0	0	0	0	138
386	373.75	0	0	0	0	0	0	291
387	373.83	0	0	0	0	0	0	342
388	373.92	0	0	0	0	0	0	6
389	374.00	0	0	0	0	0	0	97
390	374.08	0	0	0	0	0	0	130
391	374.17	0	0	0	0	0	0	176
392	374.25	0	0	0	0	0	0	278
393	374.33	0	0	0	0	0	0	295
394	374.42	0	0	0	0	0	0	330
395	374.50	0	0	0	0	0	0	18
396	374.58	0	0	0	0	0	0	140
397	374.67	0	0	0	0	0	0	180
398	374.75	0	0	0	0	0	0	279
399	374.83	0	0	0	0	0	0	328
400	374.92	0	0	0	0	0	0	351
401	375.00	0	0	0	0	0	0	26
402	375.08	0	0	0	0	0	0	82
403	375.17	0	0	0	0	0	0	111
404	375.25	0	0	0	0	0	0	104
405	375.33	0	0	0	0	0	0	26

BT#	YearDay	Hr	Lr	Qb	Qbdir	Cavg	Qs	Cdir
406	375.42	0	0	0	0	0	0	8
407	375.50	0	0	0	0	0	0	24
408	375.58	0	0	0	0	0	0	79
409	375.67	0	0	0	0	0	0	105
410	375.75	0	0	0	0	0	0	81
411	375.83	0	0	0	0	0	0	19
412	375.92	0	0	0	0	0	0	19
413	376.00	0	0	0	0	0	0	64
414	376.08	0	0	0	0	0	0	94
415	376.17	0	0	0	0	0	0	130
416	376.25	0	0	0	0	0	0	147
417	376.33	0	0	0	0	0	0	161
418	376.42	0	0	0	0	0	0	214
419	376.50	0	0	0	0	0	0	203
420	376.58	0	0	0	0	0	0	143
421	376.67	0	0	0	0	0	0	174
422	376.75	0	0	0	0	0	0	195
423	376.83	0	0	0	0	0	0	237
424	376.92	0	0	0	0	0	0	249
425	377.00	0	0	0	0	0	0	223
426	377.08	0	0	0	0	0	0	203
427	377.17	0	0	0	0	0	0	201
428	377.25	0	0	0	0	0	0	214
429	377.33	0	0	0	0	0	0	265
430	377.42	0	0	0	0	0	0	283
431	377.50	0	0	0	0	0	0	319
432	377.58	0	0	0	0	0	0	343
433	377.67	0	0	0	0	0	0	62
434	377.75	0	0	0	0	0	0	42
435	377.83	0	0	0	0	0	0	353
436	377.92	0	0	0	0	0	0	355
437	378.00	0	0	0	0	0	0	12
438	378.08	0	0	0	0	0	0	30
439	378.17	0	0	0	0	0	0	54
440	378.25	0	0	0	0	0	0	60
441	378.33	0	0	0	0	0	0	42
442	378.42	0	0	0	0	0	0	40
443	378.50	0	0	0	0	0	0	59
444	378.58	0	0	0	0	0	0	95
445	378.67	0	0	0	0	0	0	140
446	378.75	0	0	0	0	0	0	152
447	378.83	0	0	0	0	0	0	179
448	378.92	0	0	0	0	0	0	222
449	379.00	0	0	0	0	0	0	261
450	379.08	0	0	0	0	0	0	215
451	379.17	0	0	0	0	0	0	166
452	379.25	0	0	0	0	0	0	140
453	379.33	0	0	0	0	0	0	48
454	379.42	0	0	0	0	0	0	152
455	379.50	0	0	0	0	0	0	256
456	379.58	0	0	0	0	0	0	249
457	379.67	0	0	0	0	0	0	230
458	379.75	0	0	0	0	0	0	213
459	379.83	0	0	0	0	0	0	233
460	379.92	0	0	0	0	0	0	271
461	380.00	0	0	0	0	0	0	311
462	380.08	0	0	0	0	0	0	332
463	380.17	0	0	0	0	0	0	357
464	380.25	0	0	0	0	0	0	51
465	380.33	0	0	0	0	0	0	198
466	380.42	0	0	0	0	0	0	313
467	380.50	0	0	0	0	0	0	360
468	380.58	0	0	0	0	0	0	349
469	380.67	0	0	0	0	0	0	73
470	380.75	0	0	0	0	0	0	88
471	380.83	0	0	0	0	0	0	63
472	380.92	0	0	0	0	0	0	79
473	381.00	0	0	0	0	0	0	75
474	381.08	2.34	15.9	0.000007	90	0	0	47
475	381.17	1.65	15.9	0.000024	39	0	0	11
476	381.25	1.82	15.9	0.000109	159	0	0	99
477	381.33	1.52	15.9	0.000193	177	0	0	127
478	381.42	2.09	15.9	0.000036	178	0	0	148
479	381.50	0	0	0	0	0	0	113
480	381.58	0	0	0	0	0	0	150
481	381.67	0	0	0	0	0	0	142
482	381.75	0	0	0	0	0	0	136
483	381.83	0	0	0	0	0	0	150
484	381.92	0	0	0	0	0	0	192